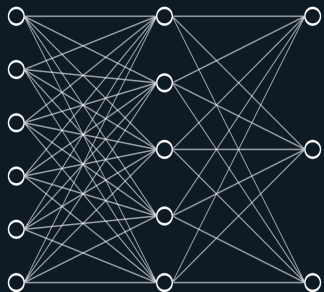
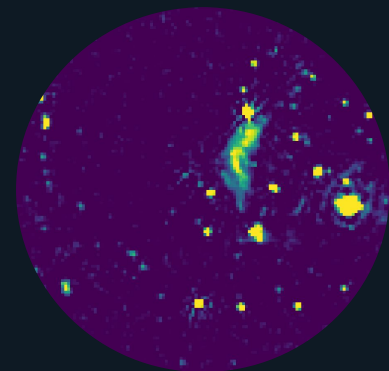


# Classification of diffuse radio emission from LoTSSDR2



Markus Bredberg  
26th of January 2026  
Supervisor: Emma Tolley

SKACH EPFL



# Classification of diffuse radio emission from LoTSSDR2



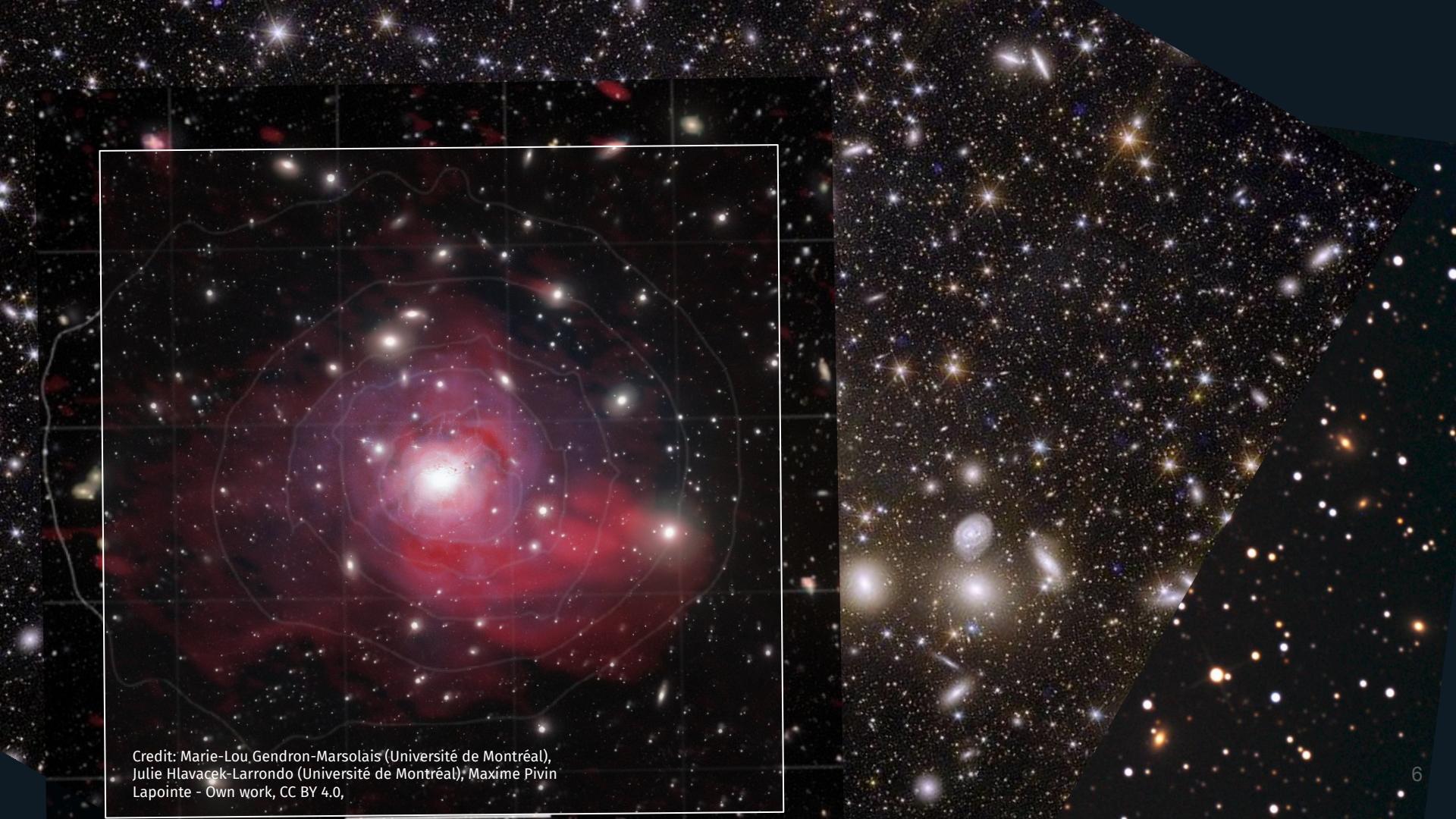
# Classification of diffuse radio emission from LoTSSDF2



Credit: J.-C. Cuillandre,  
Euclid, ESA, NASA



Credit: radio: VLA 230–470 MHz, Gendron-Marsolais+17;  
optical: SDSS, gri bands, Abolfathi+18



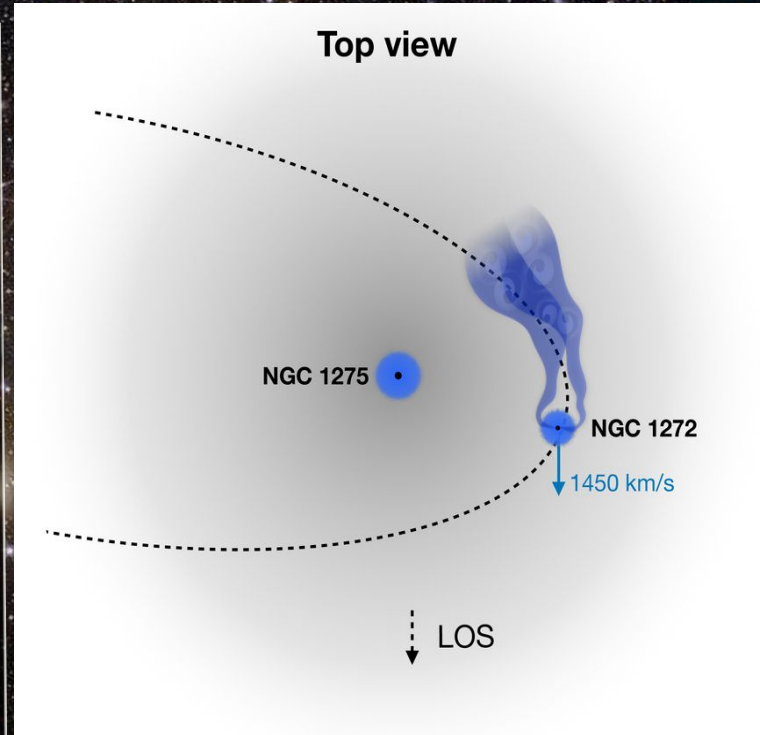
Credit: Marie-Lou Gendron-Marsolais (Université de Montréal),  
Julie Hlavacek-Larrondo (Université de Montréal), Maxime Pivin  
Lapointe - Own work, CC BY 4.0,



Credit: Gendron-Marsolais et al 2021 ApJ 914

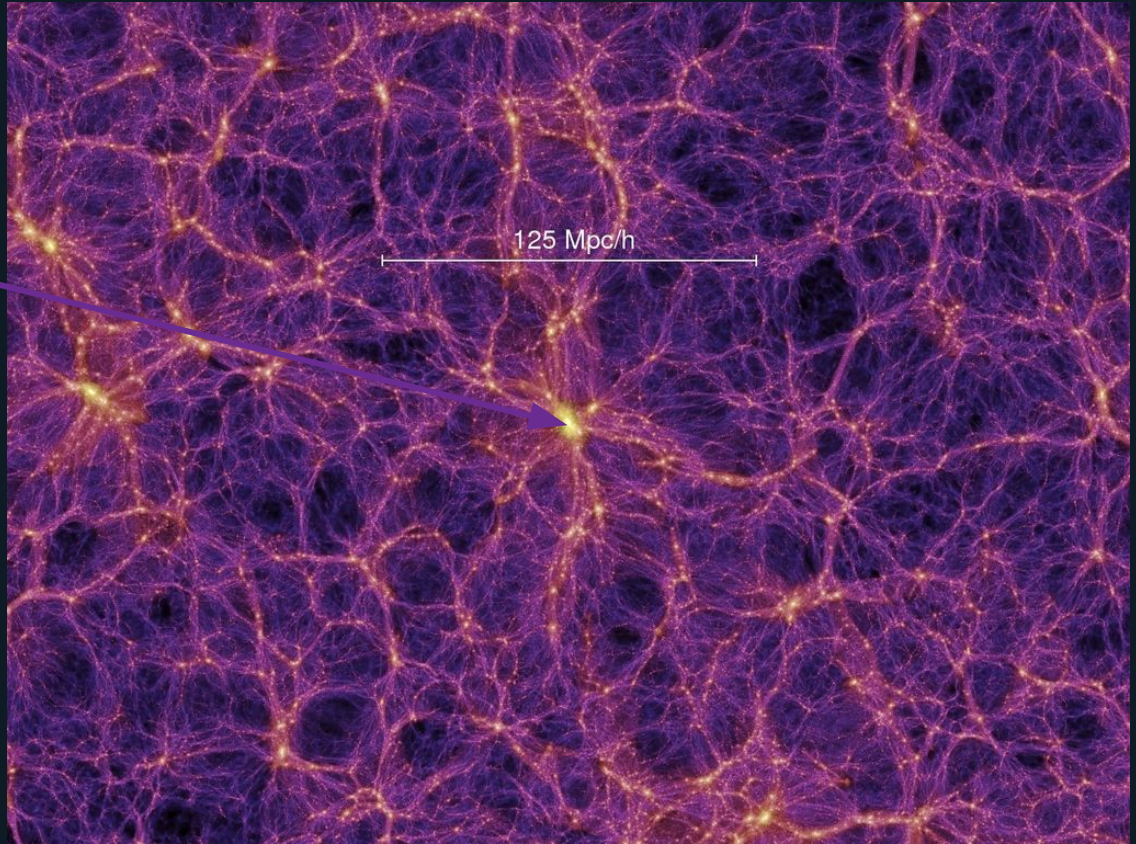


Credit: Gendron-Marsolais et al 2021 ApJ 914



# The presence of large-scale magnetic fields

Galaxy clusters:  $\sim \mu\text{G}$

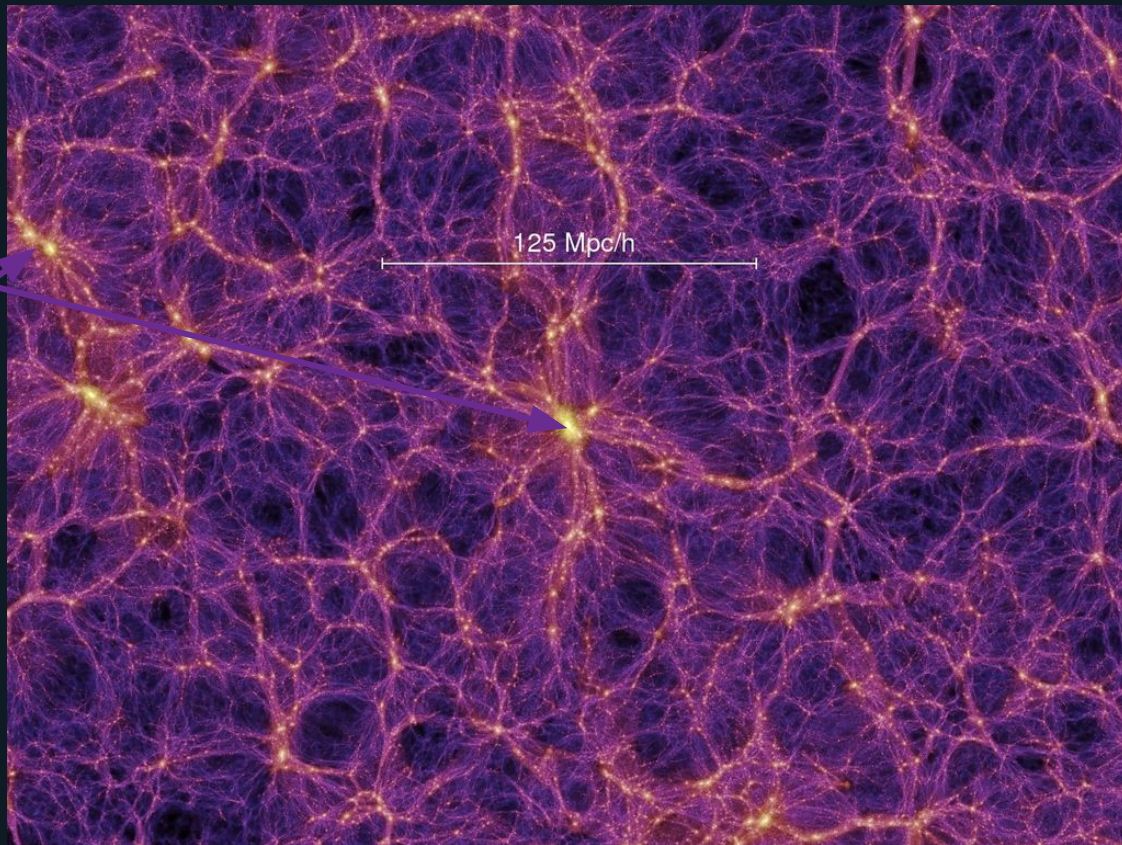


Credit: Millennium run

# The presence of large-scale magnetic fields

Galaxy clusters:  $\sim \mu\text{G}$

Intercluster bridges:  $\sim .1 \mu\text{G}$



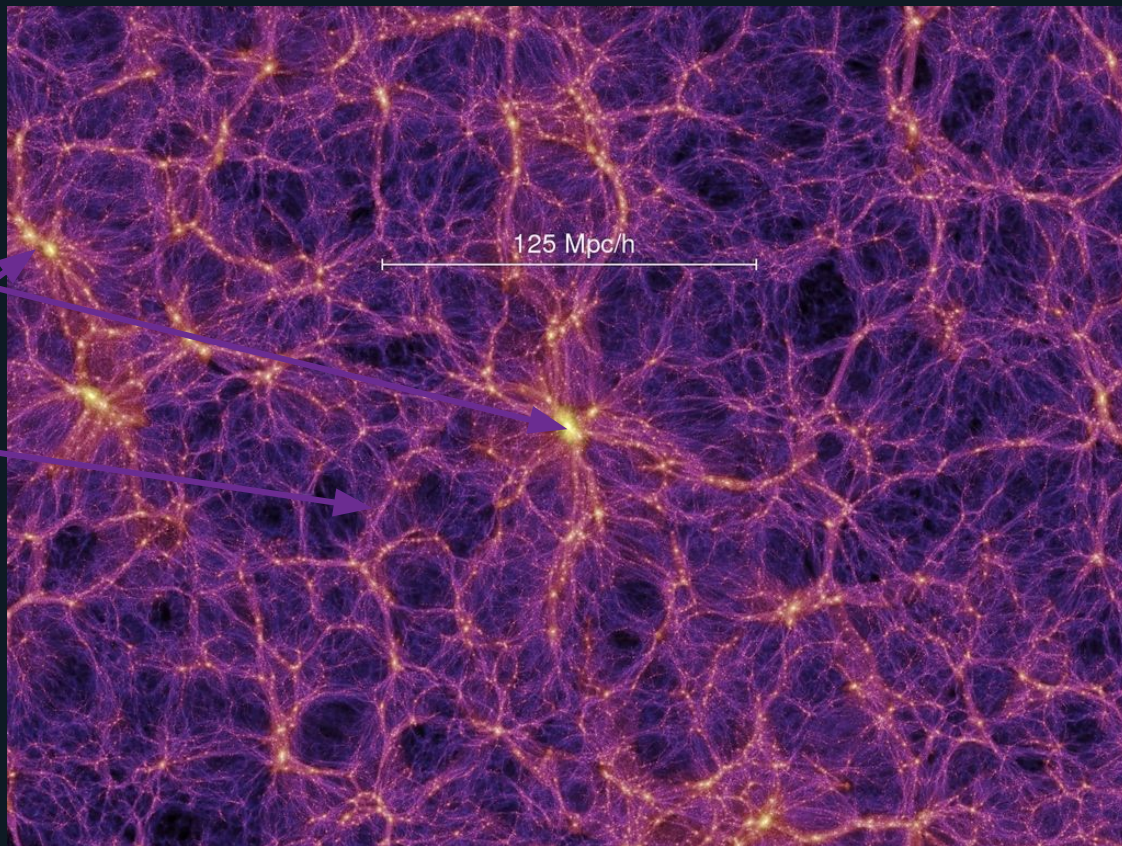
Credit: Millennium run

# The presence of large-scale magnetic fields

Galaxy clusters:  $\sim \mu\text{G}$

Intercluster bridges:  $\sim .1\mu\text{G}$

Cosmic filaments:  $< \text{nG}$



Credit: Millennium run

# The presence of large-scale magnetic fields

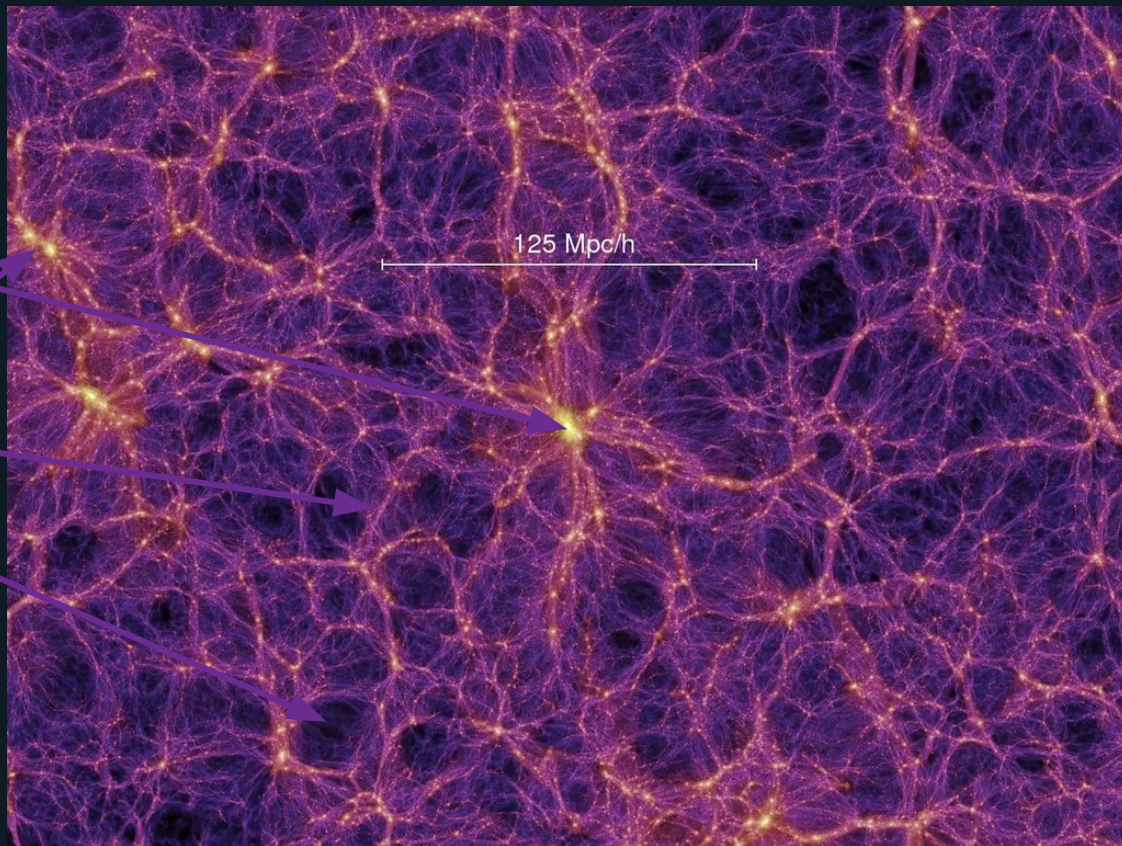
$$\beta = p_{\text{thermal}} / p_{\text{magnetic}} \sim 100$$

Galaxy clusters:  $\sim \mu\text{G}$

Intercluster bridges:  $\sim .1 \mu\text{G}$

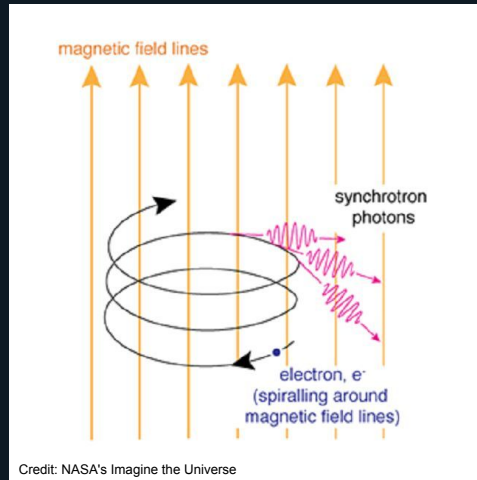
Cosmic filaments:  $< \text{nG}$

Cosmic voids:  $10^{-16} - 10^{-10}?$



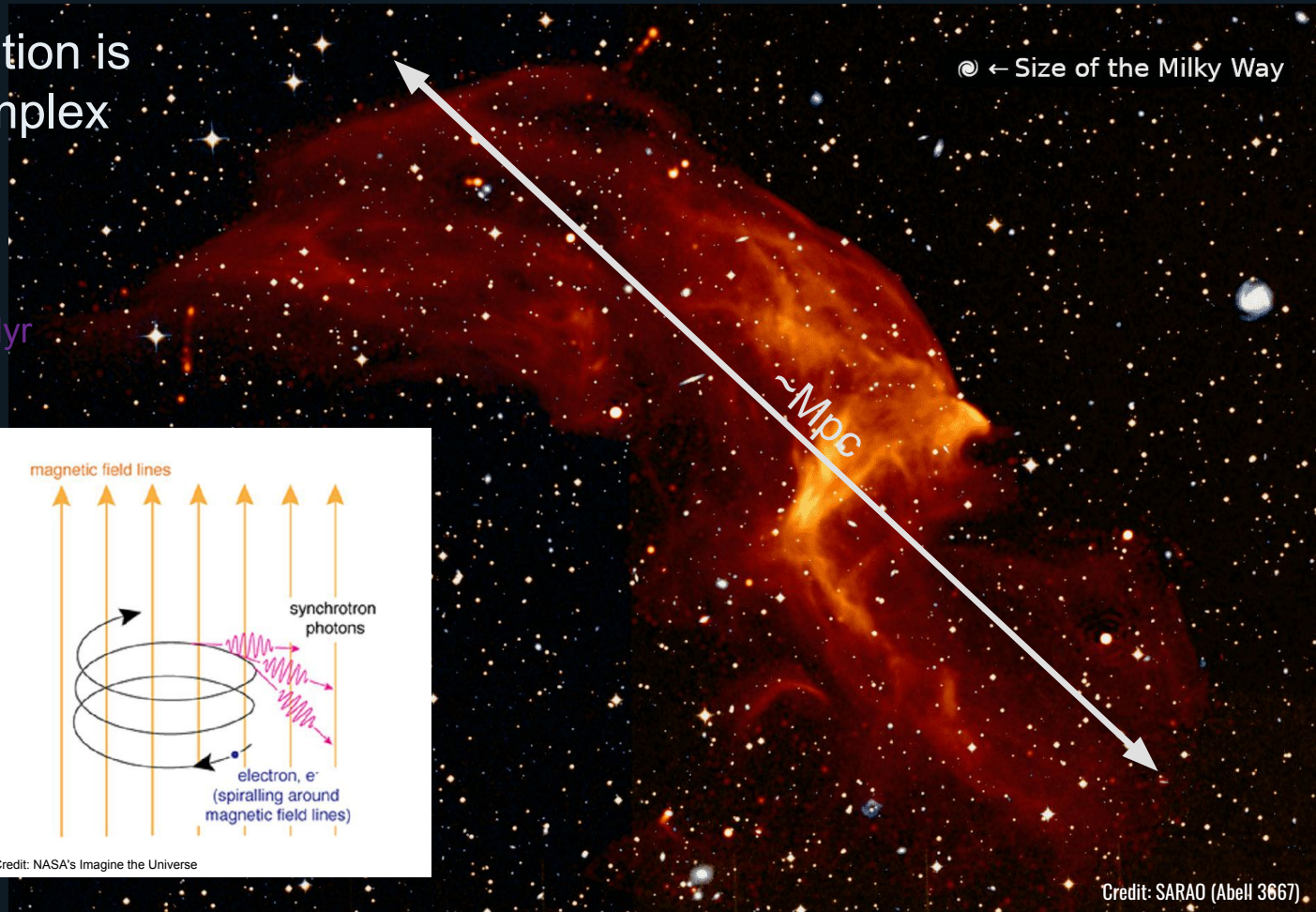
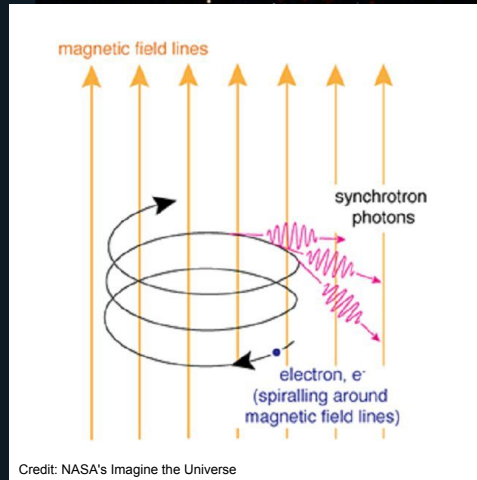
Credit: Millennium run

# Synchrotron radiation is extended and complex



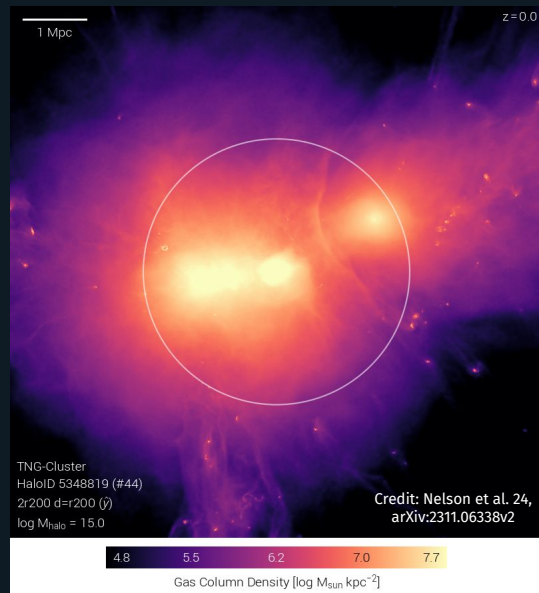
# Synchrotron radiation is extended and complex

Time to cover: ~Gyr  
Dissipation time: ~10-100 Myr  
→ In-situ re-acceleration



Credit: SARAO (Abell 3667)

## Galaxy cluster mergers are extremely energetic



Rotation



Turbulence

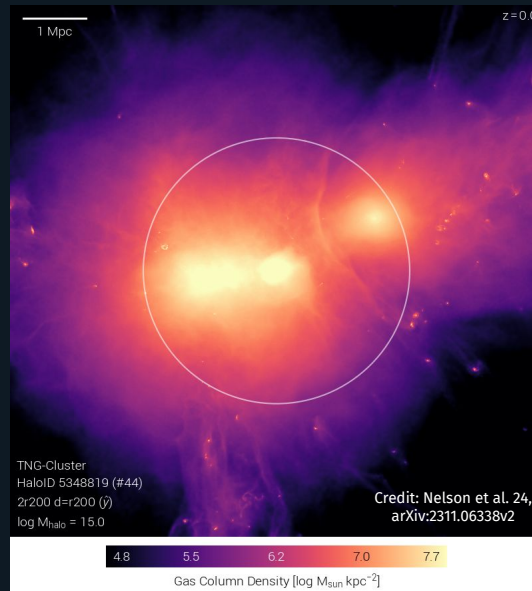


Gas  
compression



Magnetic  
field growth

# Galaxy cluster mergers are extremely energetic



Rotation



Turbulence



Gas  
compression

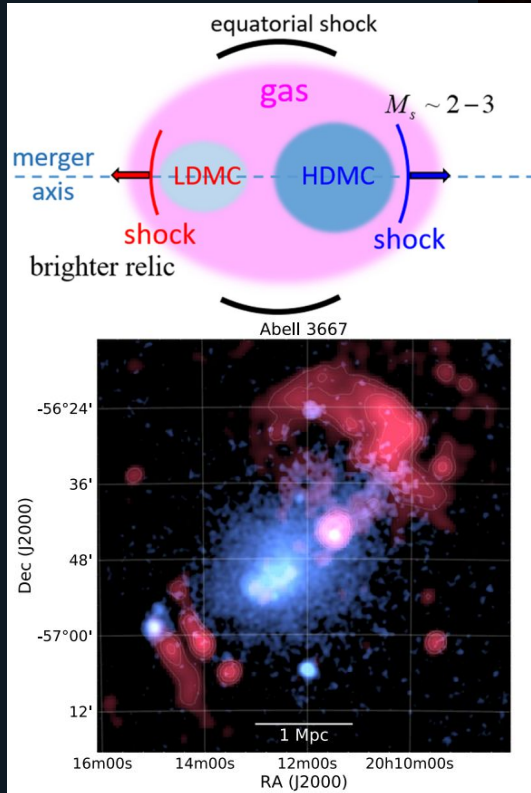


Magnetic  
field growth

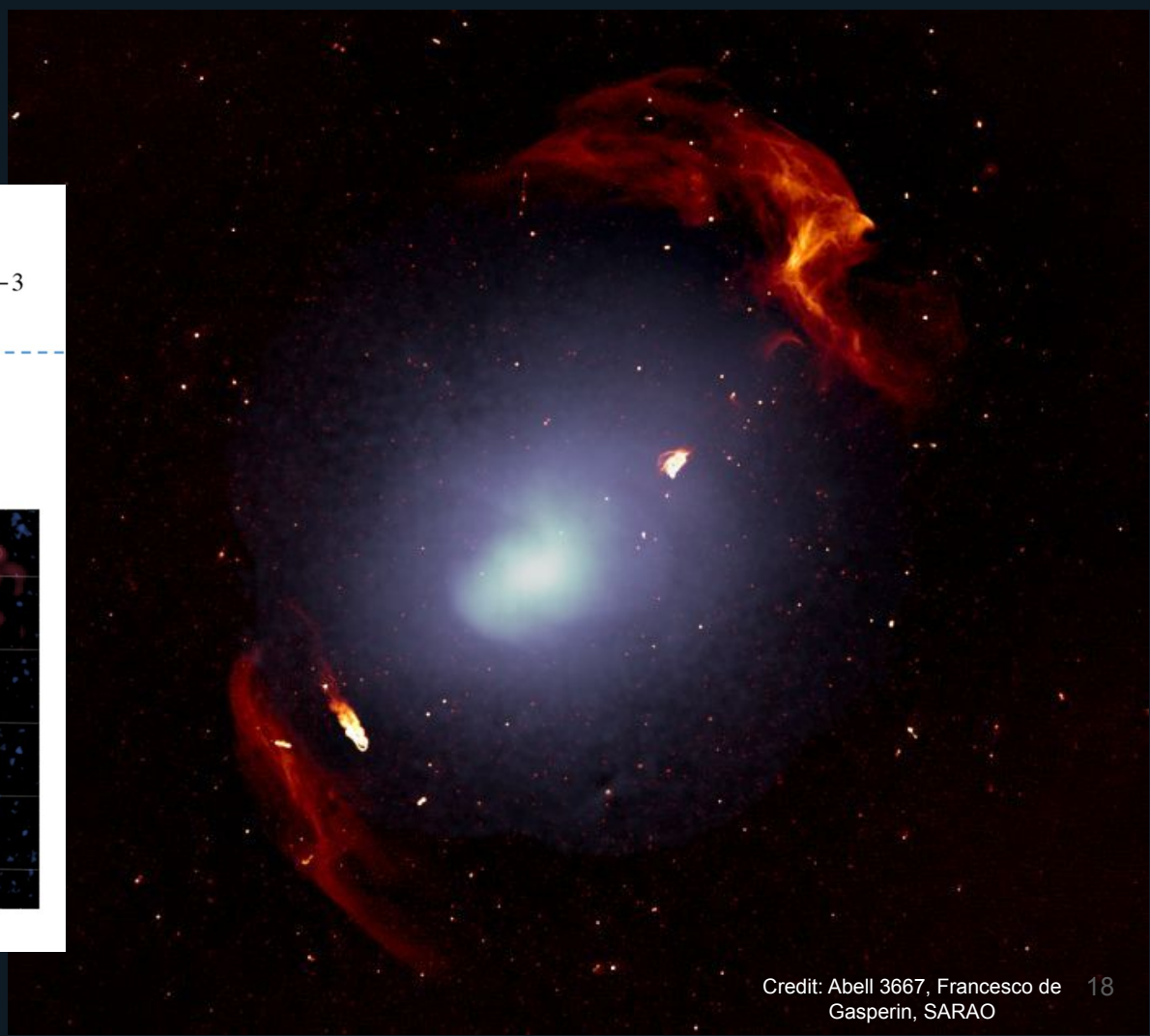
Radio relics are shock-accelerated



# Radio relics are shock-accelerated



Credit: MWA 170–231 MHz and ROSAT PSPC  
(Hurley-Walker et al. 2017; Voges et al. 1999)

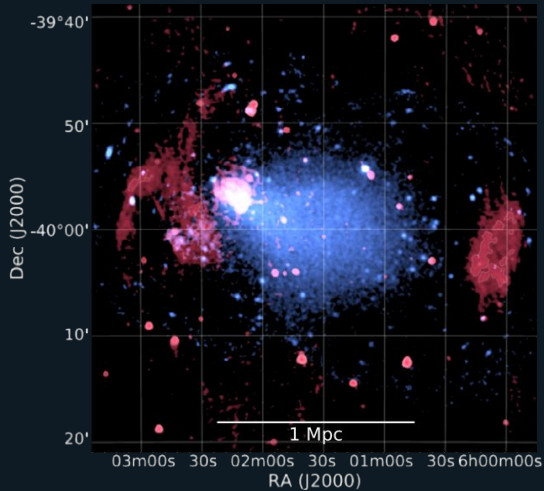


Credit: Abell 3667, Francesco de Gasperin, SARAO 18

# Classification of diffuse radio emission from LoTSSDR2

# Synchrotron radiation probes relativistic charged particles and magnetic fields

## Radio Relic



MWA 170–231 MHz and ROSAT PSPC (Hurley-Walker et al. 2017; Voges et al. 1999)

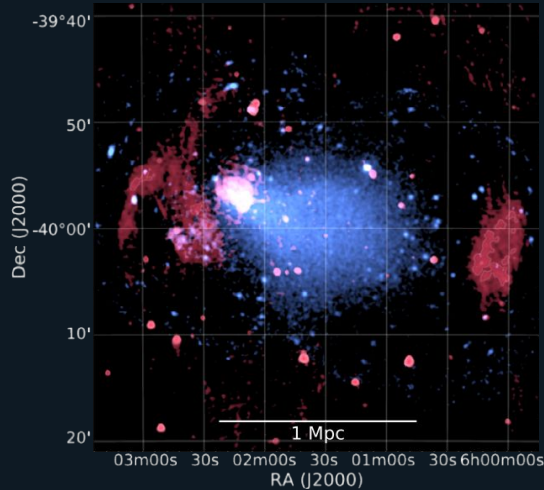
Periphery in merger

$\approx 1$  Mpc

$\sim 30\text{-}70\%$  polarisation

# Synchrotron radiation probes relativistic charged particles and magnetic fields

## Radio Relic



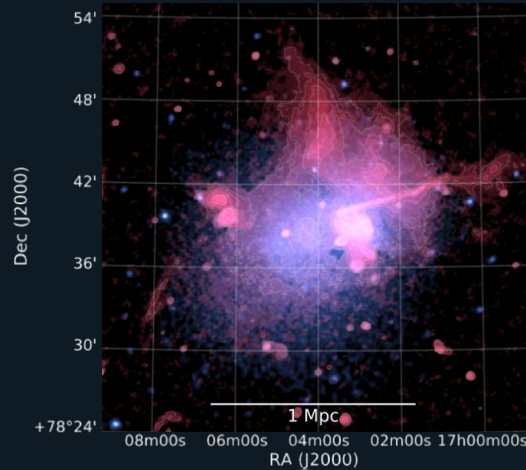
MWA 170–231 MHz and ROSAT PSPC (Hurley-Walker et al. 2017; Voges et al. 1999)

Periphery in merger

$\approx 1$  Mpc

$\sim 30\text{-}70\%$  polarisation

## Radio Halo



LOFAR 120–170 MHz and XMM-Newton 0.4–1.3 keV (van Weeren et al. in prep)

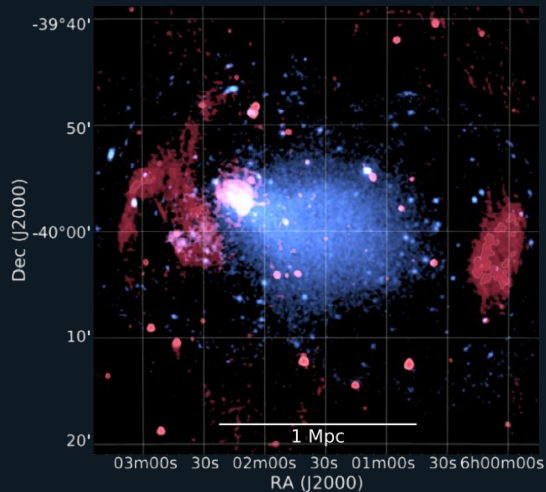
Centre of cluster

$\sim 300$  kpc to  $\sim 2$  Mpc

Large cluster mass

# Synchrotron radiation probes relativistic charged particles and magnetic fields

## Radio Relic



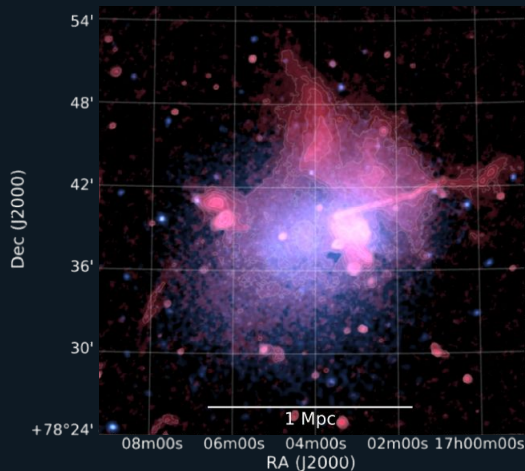
MWA 170–231 MHz and ROSAT PSPC (Hurley-Walker et al. 2017; Voges et al. 1999)

Periphery in merger

$\approx 1$  Mpc

$\sim 30$ -70 % polarisation

## Radio Halo



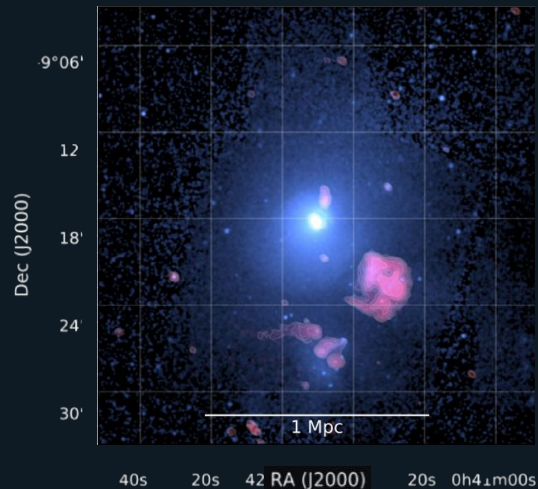
LOFAR 120–170 MHz and XMM-Newton 0.4–1.3 keV (van Weeren et al. in prep)

Centre of cluster

$\sim 300$  kpc to  $\sim 2$  Mpc

Large cluster mass

## Revived Fossil Plasma



GMRT 148 MHz and Chandra 0.5–2.0 keV (Andrade-Santos et al. 2017)

Anywhere in cluster

$\sim 300$  kpc

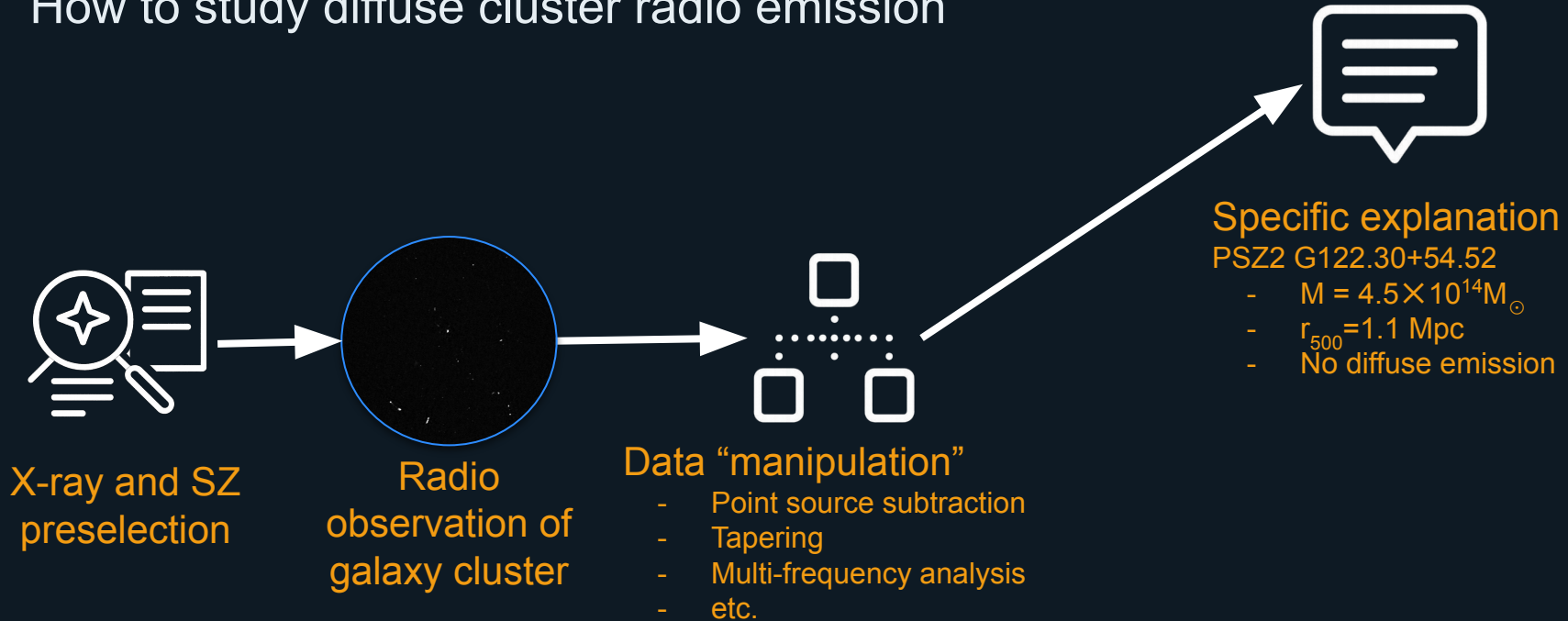
AGN origin, and ultra-steep radio spectra with breaks



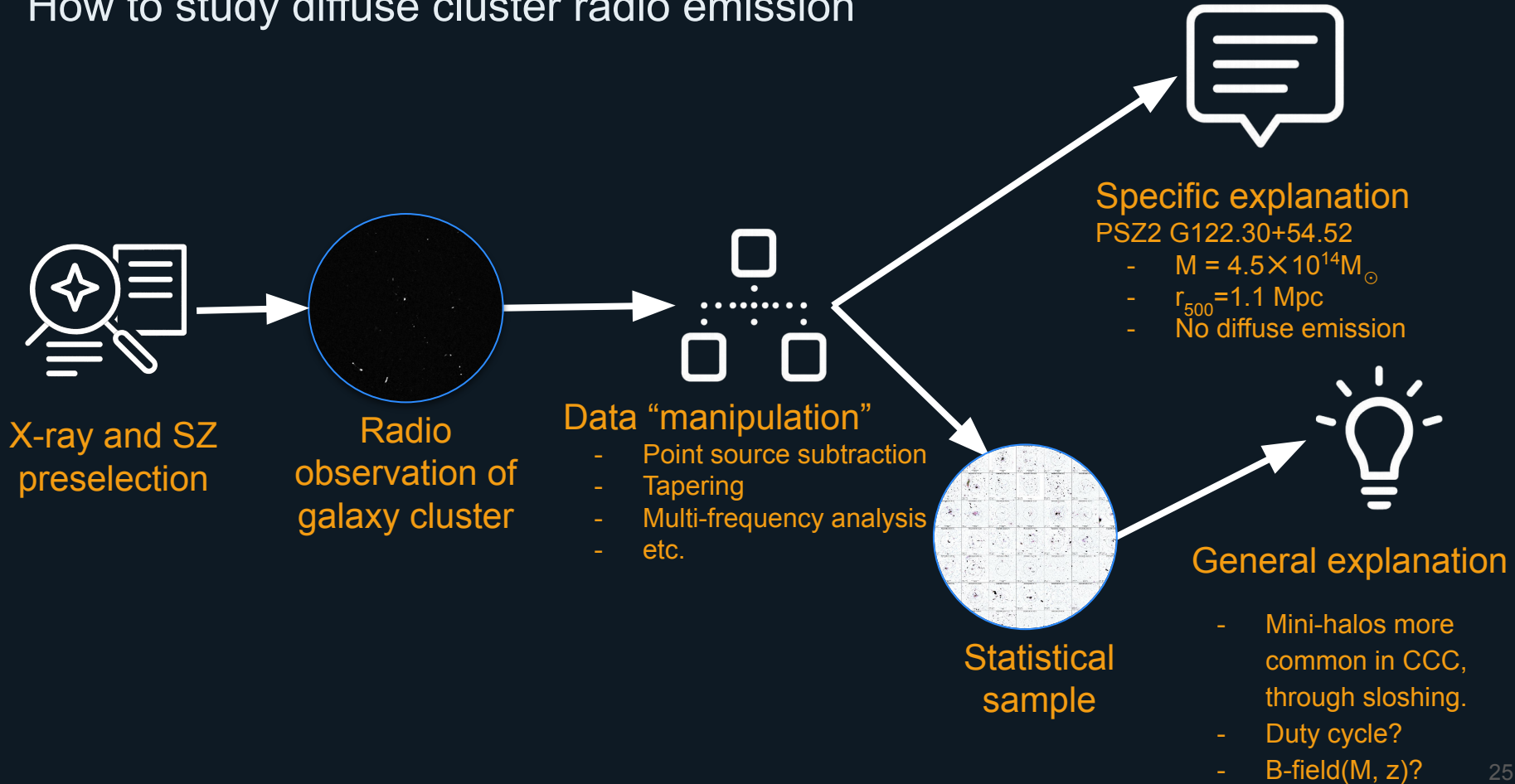
PSZ2G122.30+54  
(38.65' x 35.4')

- Growth and evolution of magnetic fields
- Cosmic-ray particle acceleration
- Dynamics, demographics and evolution of clusters

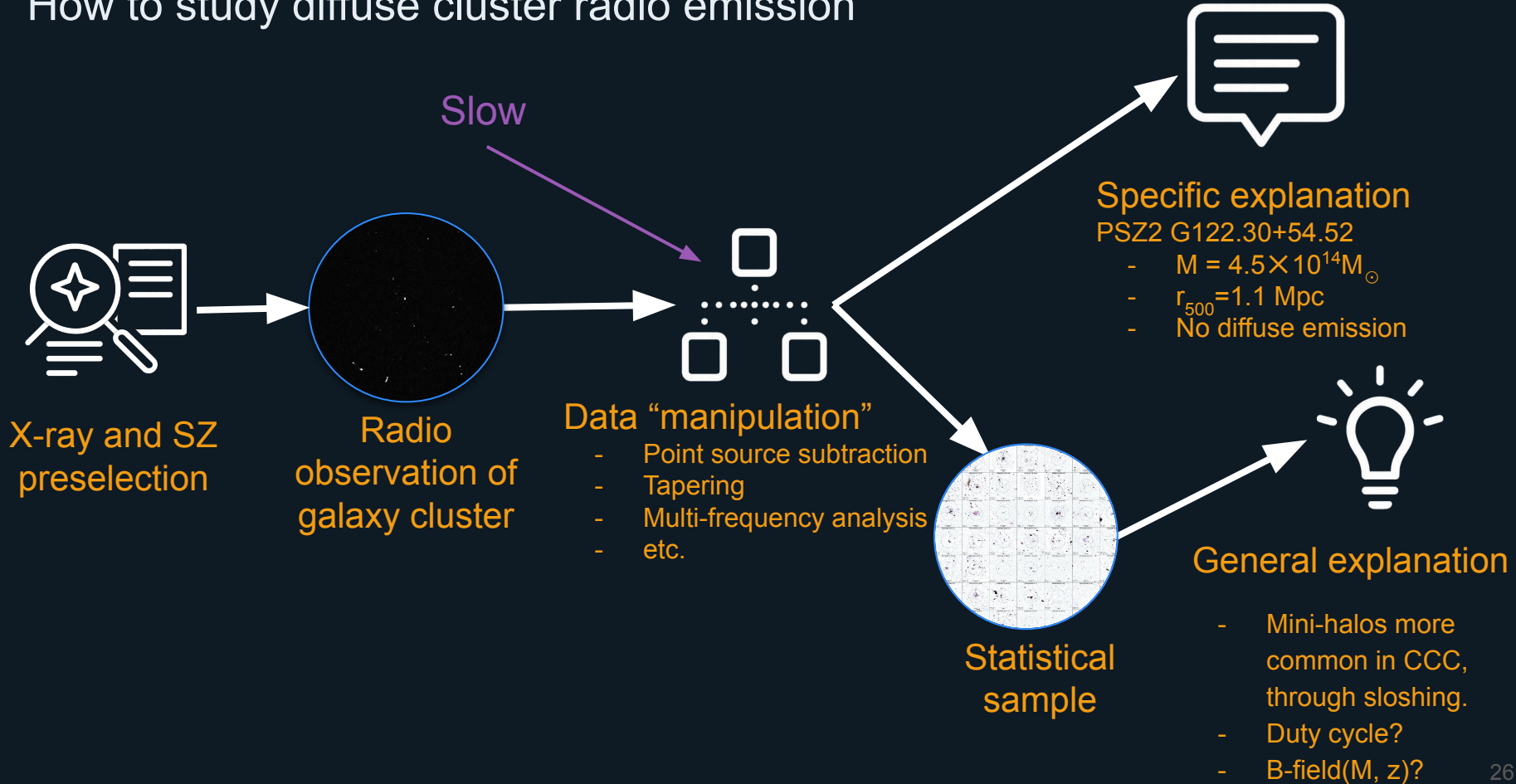
# How to study diffuse cluster radio emission



# How to study diffuse cluster radio emission



# How to study diffuse cluster radio emission

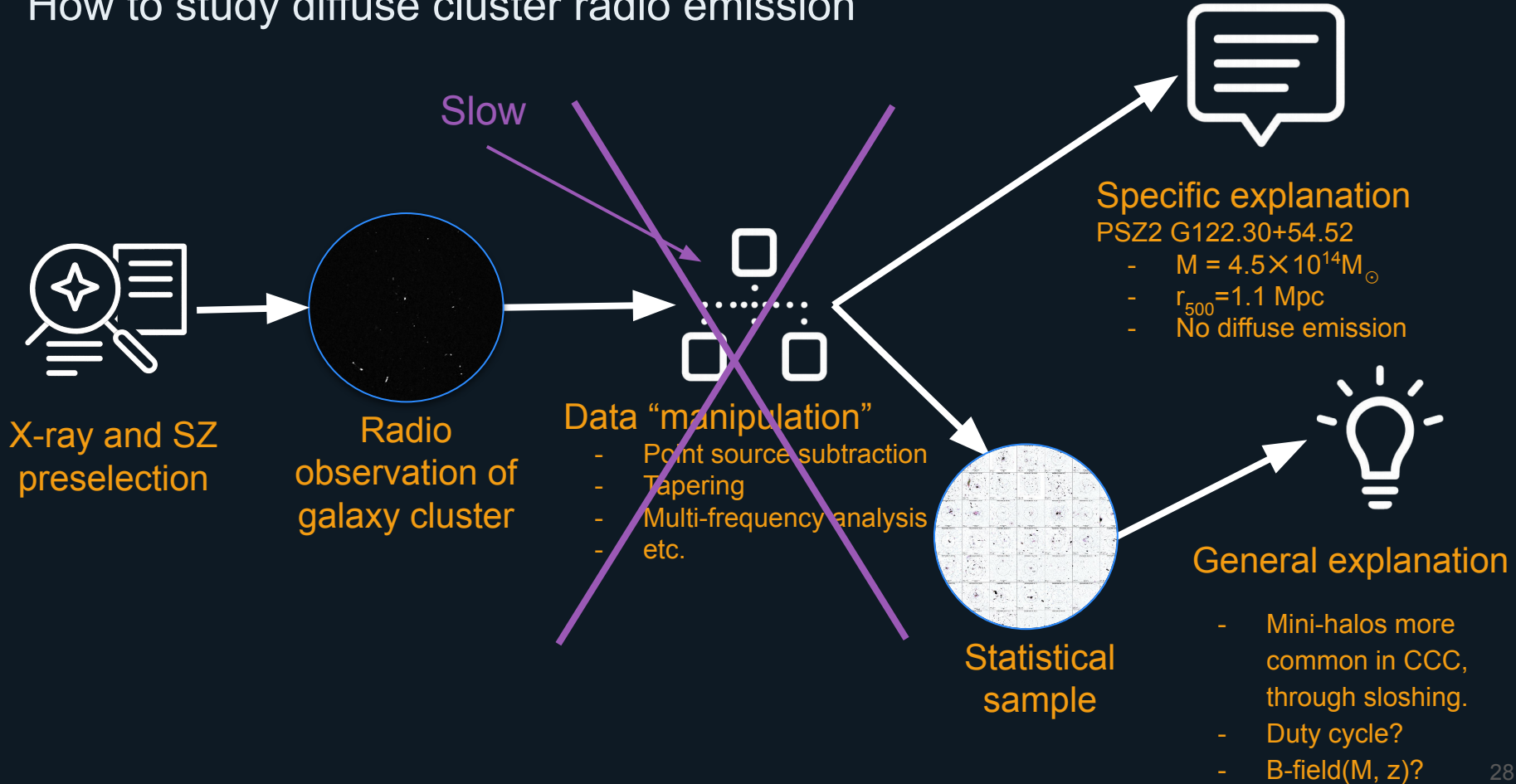


# Greater abundance calls for greater order

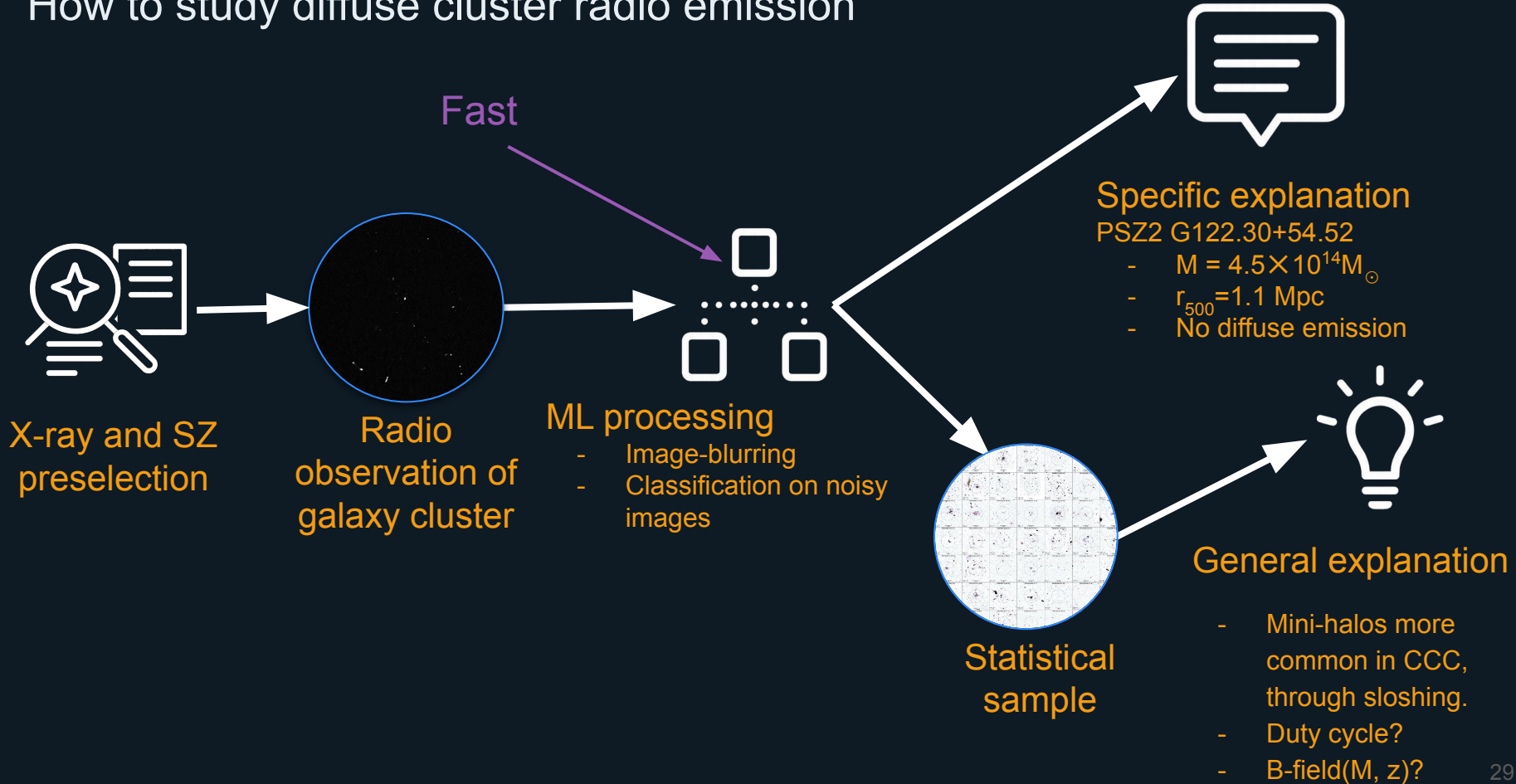


Credit: Cassano et al. 2014, [arXiv:1412.5940](https://arxiv.org/abs/1412.5940)  
Botteon et al. 2022, <https://doi.org/10.1051/0004-6361/202143020>  
SKAO 2021, SKA1 Scientific Use Cases (Rev. 04)  
Gitti et al. 2018, <https://doi.org/10.1051/0004-6361/2018327>

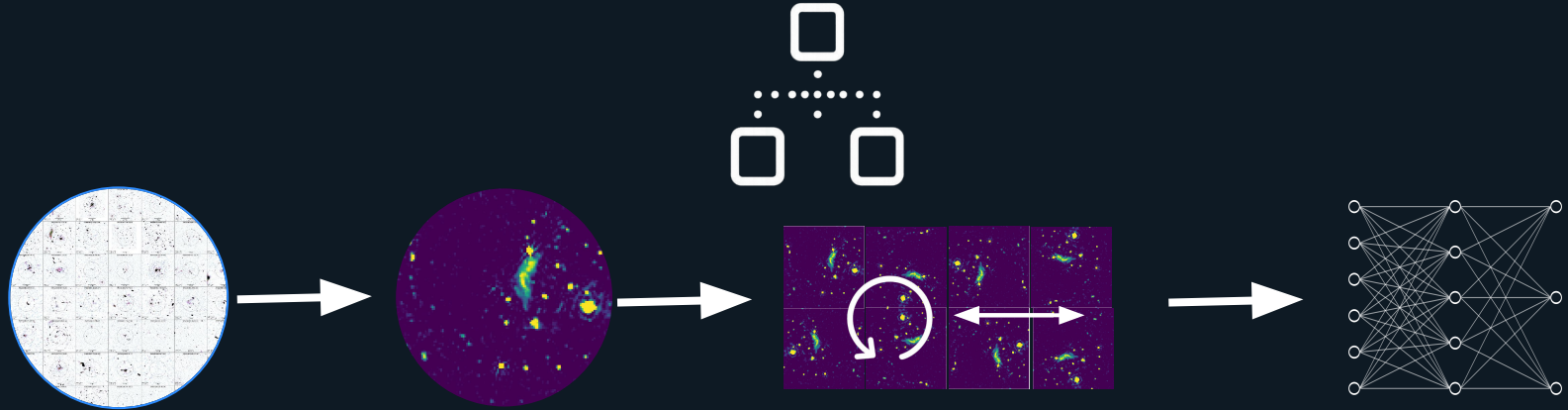
# How to study diffuse cluster radio emission



# How to study diffuse cluster radio emission



# Machine learning processing



## Acquired data

## Preprocess

- Cropping
- Downsampling
- Normalisation
- Tapering

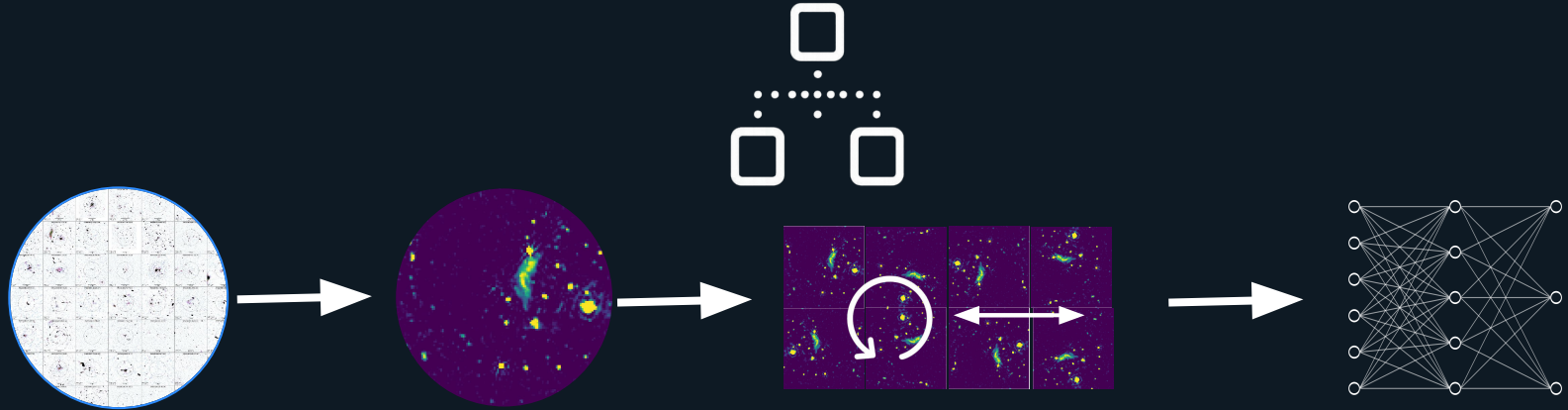
## Classical augmentation

- Flipping
- Rotations

## Classification

- Feature extraction
  - Scattering transform
  - Squeeze-excitation
- Feature correlations

# Machine learning processing



Acquired data

Preprocess

- Cropping
- Downsampling
- Normalisation
- Tapering

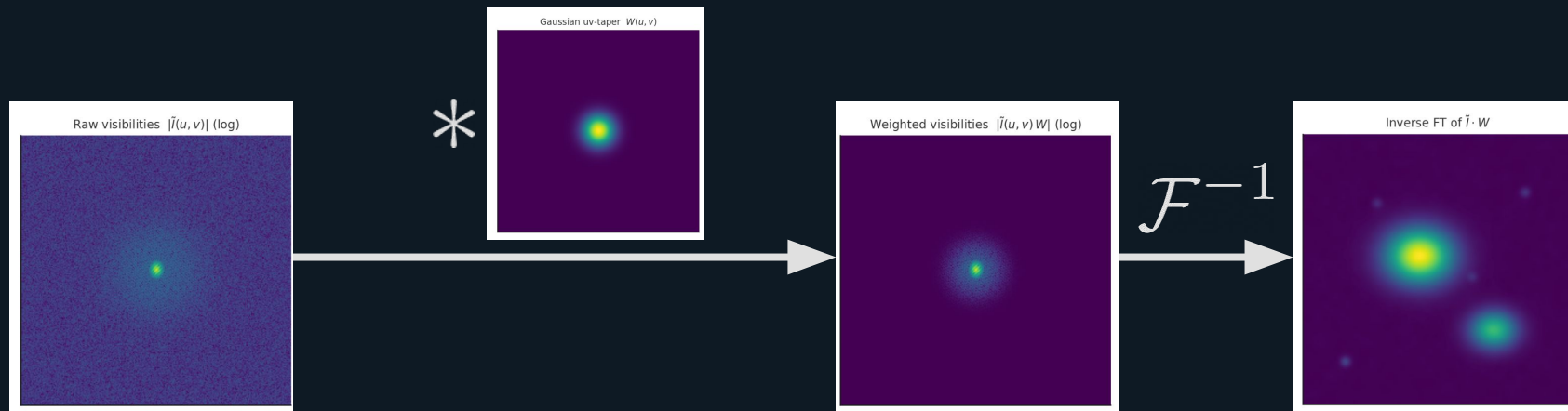
Classical augmentation

- Flipping
- Rotations

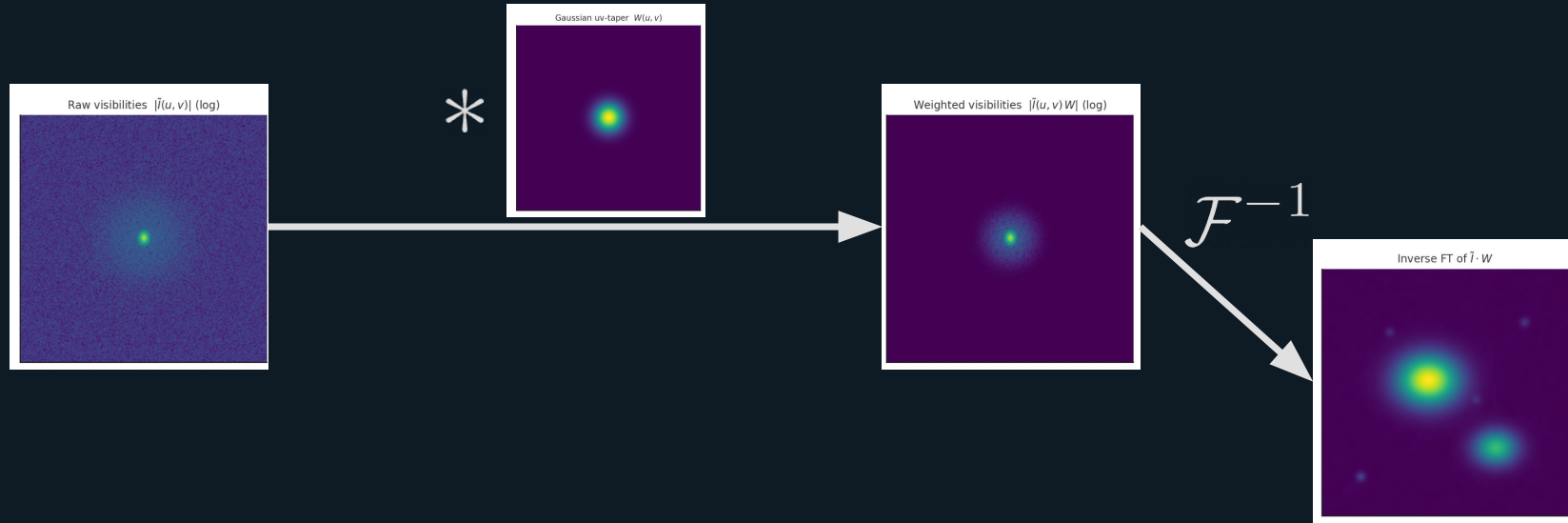
Classification

- Feature extraction
  - Scattering transform
  - Squeeze-excitation
- Feature correlations

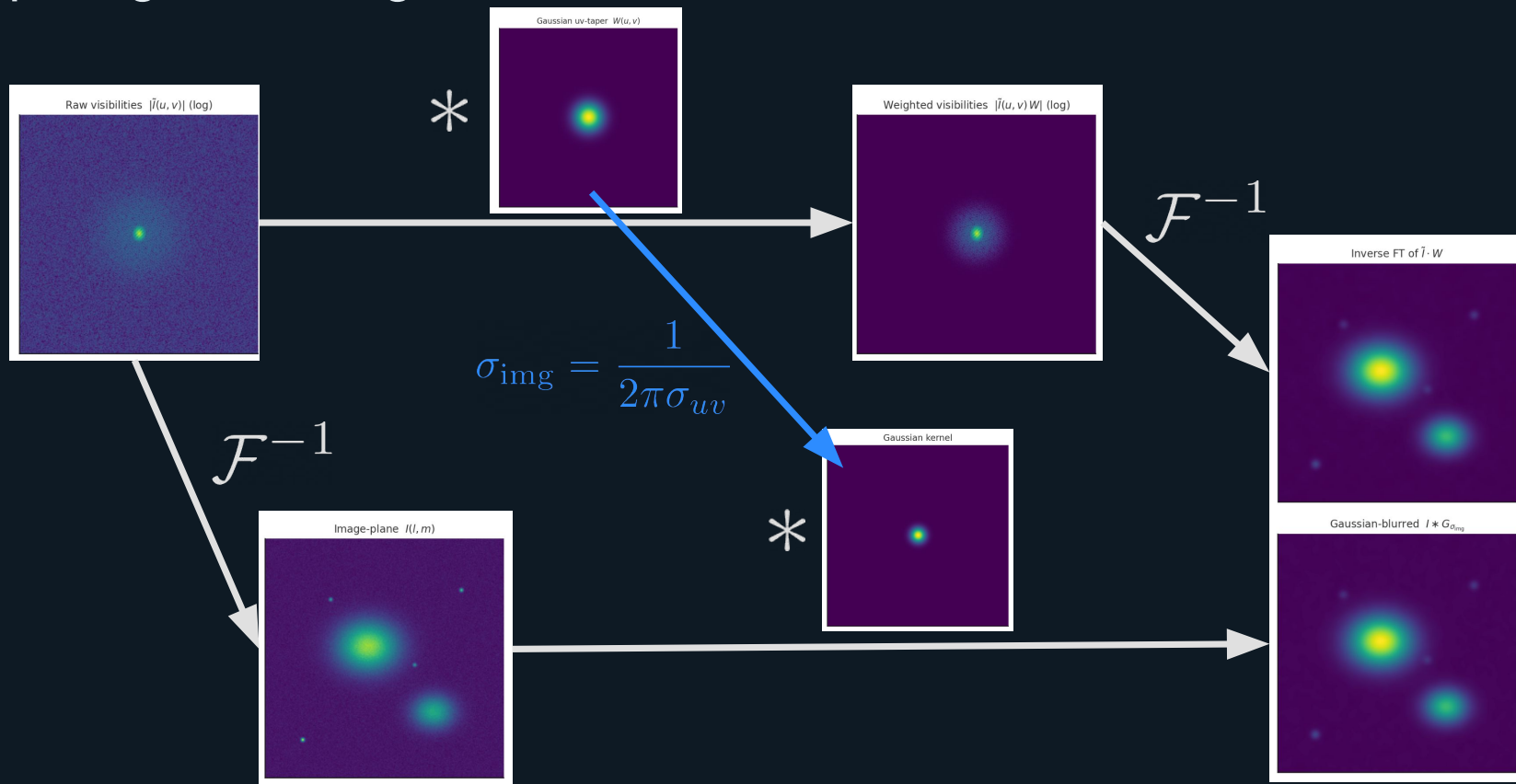
# Tapering downweights longer baselines



# Tapering downweights smaller scales



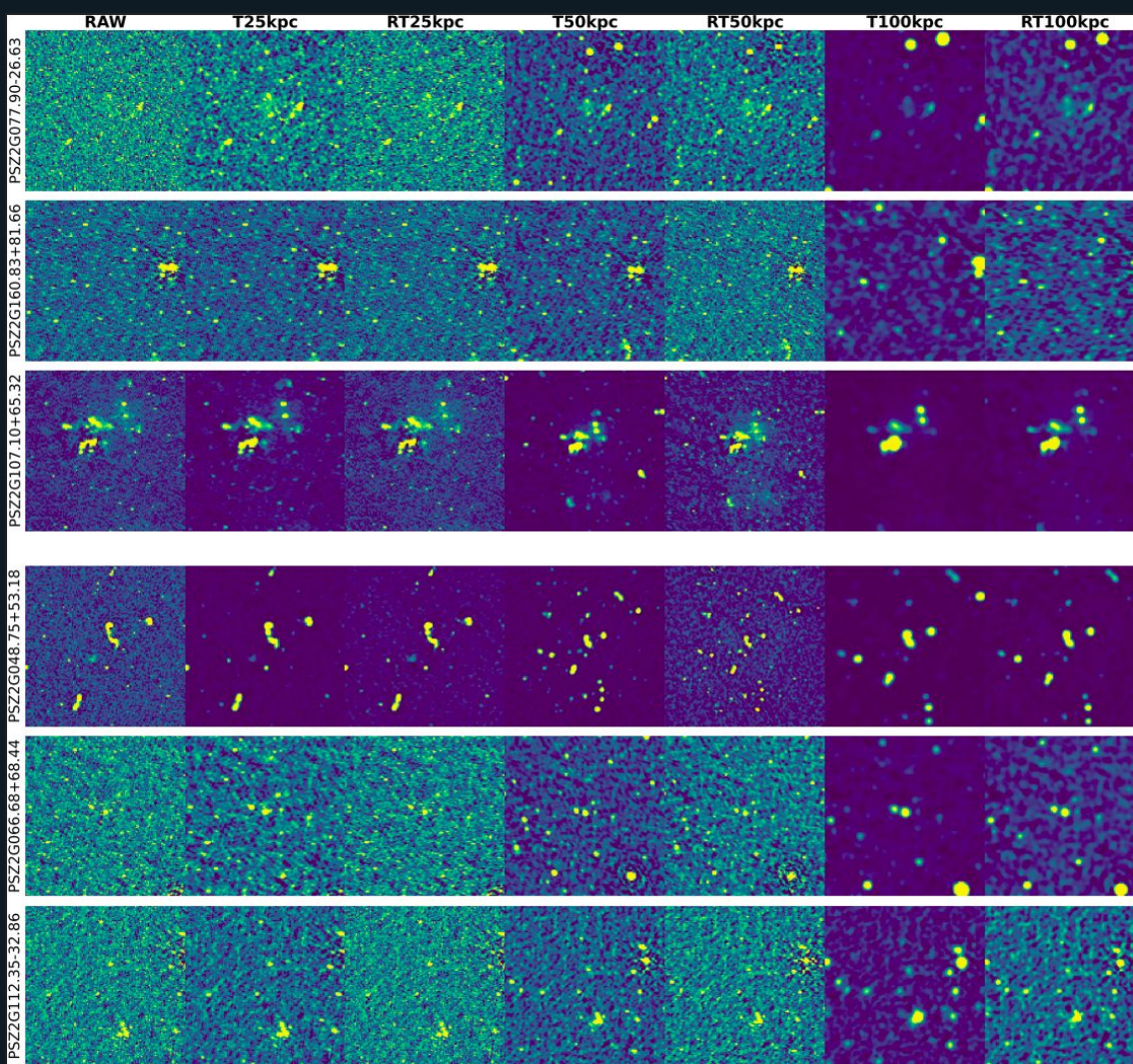
# Tapering downweights smaller scales



Blurring almost reproduces tapering

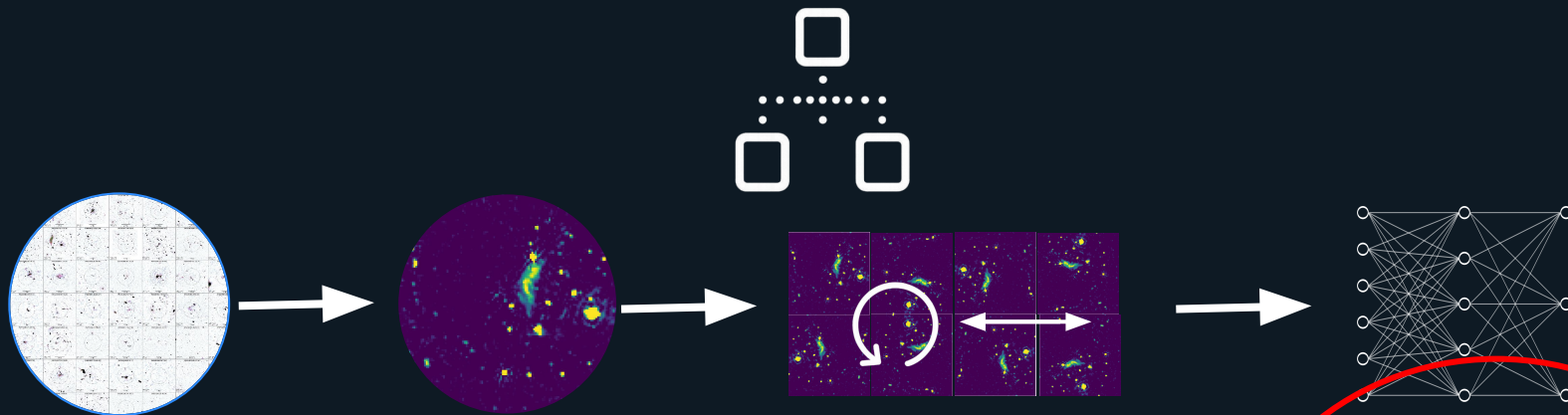
Diffuse emission

No diffuse emission



RT = blurring of image  
T = tapering of visibilities

# Machine learning processing



## Acquired data

## Preprocess

- Cropping
- Downsampling
- Normalisation
- Tapering

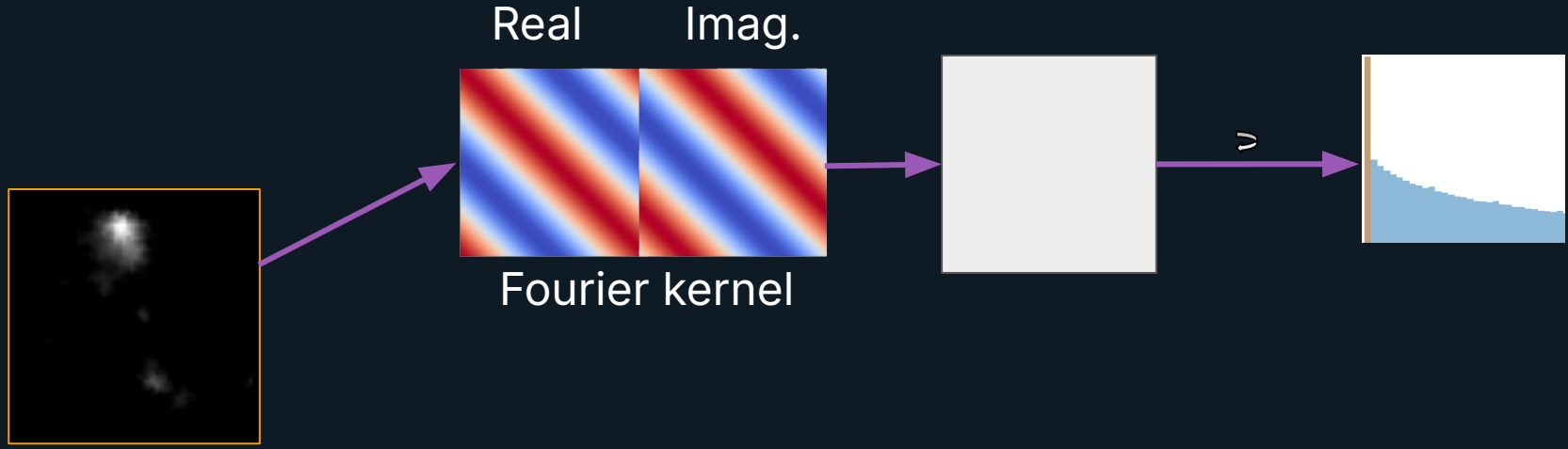
## Classical augmentation

- Flipping
- Rotations

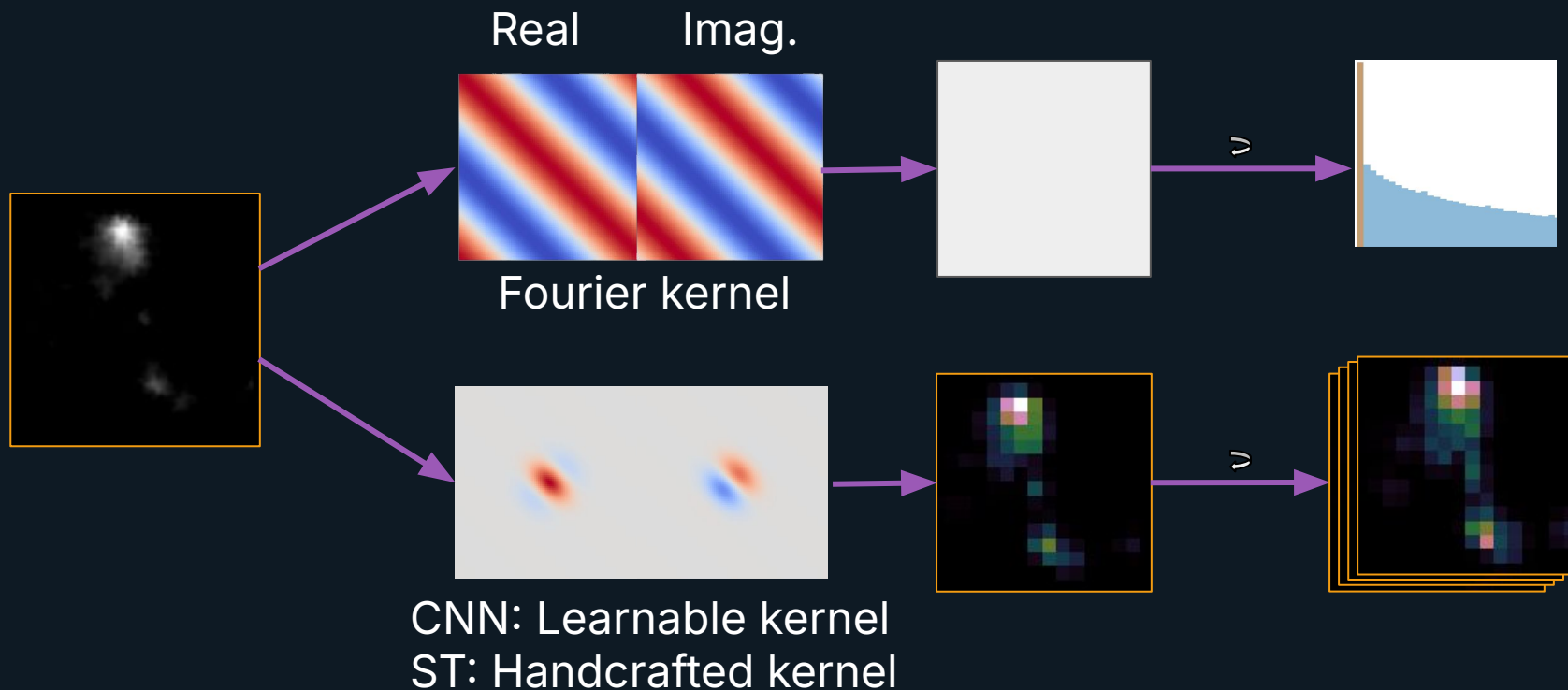
## Classification

- Feature extraction
  - Scattering transform
  - Squeeze-excitation
- Feature correlations

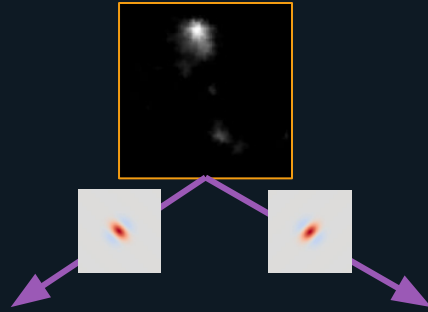
# Kernels are localised and extract spatial information



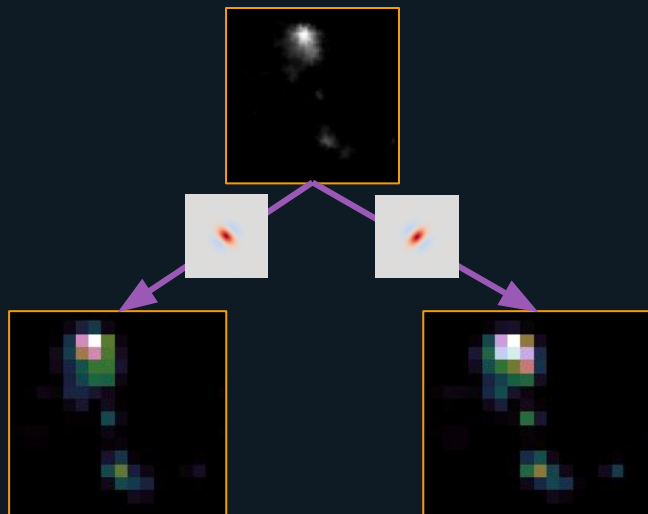
# Kernels are localised and extract spatial information



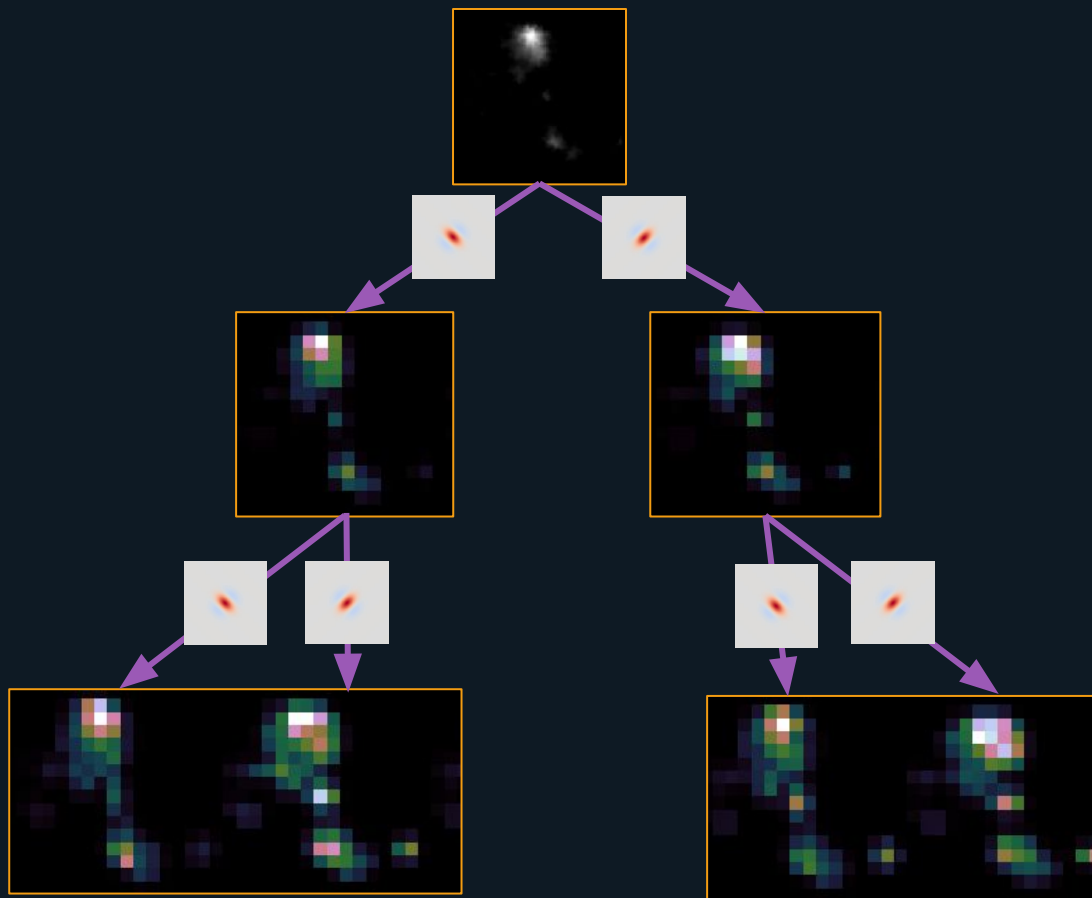
The scattering transform iteratively applies a wavelet transform



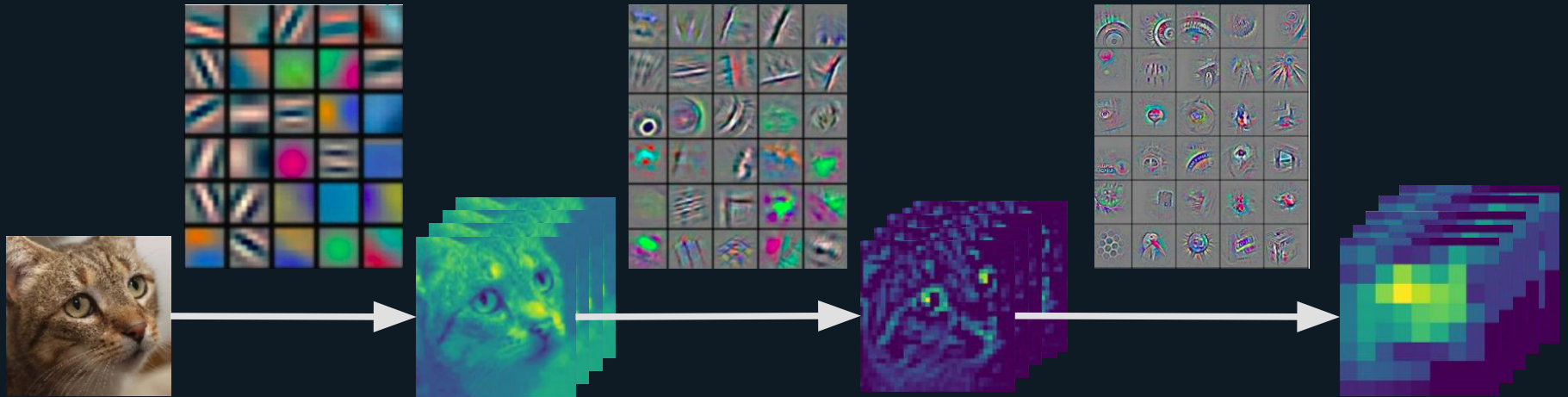
The scattering transform iteratively applies a wavelet transform



The scattering transform iteratively applies a wavelet transform

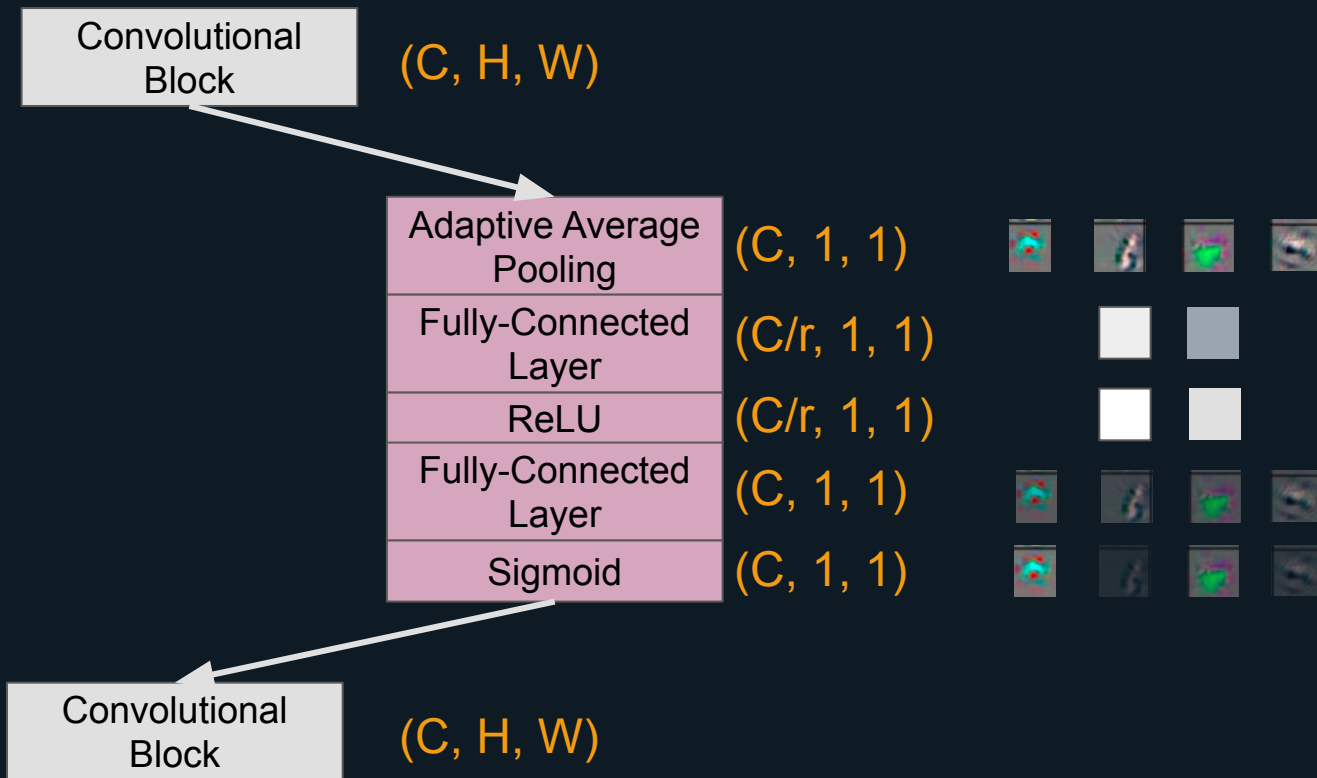


# A convolutional neural network (CNN) extracts features



Credit: <https://stackoverflow.com/questions/38450104/how-to-visualize-filters-after-the-1st-layer-trained-by-cnns> [edited]

# Squeeze-excitation attention weighs the channels



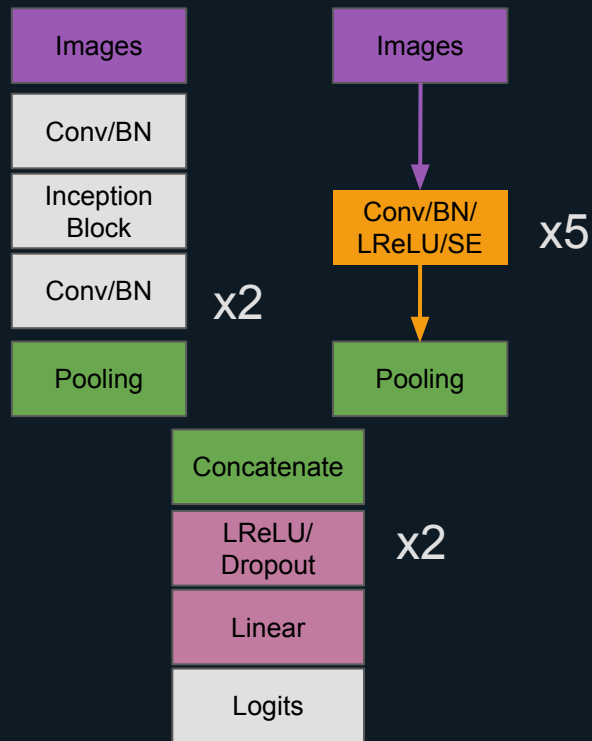
# Convolutional neural network (CNN)



## Convolutional neural network (CNN)



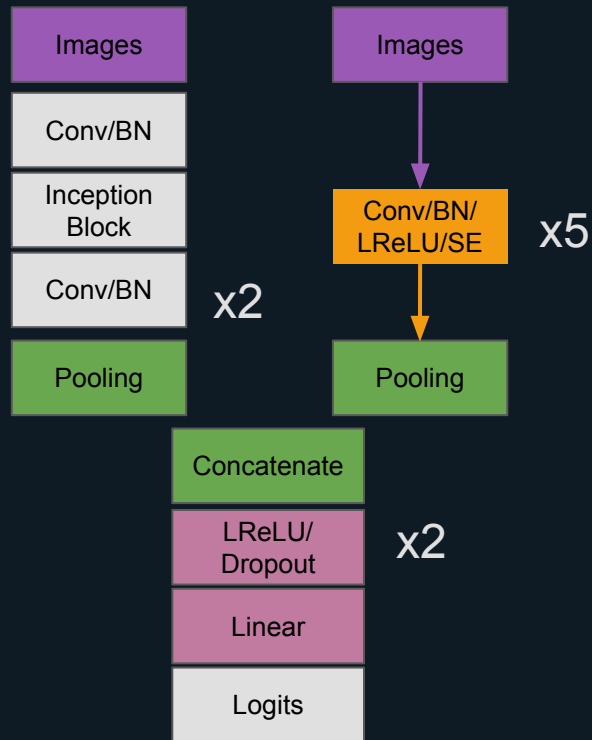
## CNN-squeeze dual net (DualCSN)



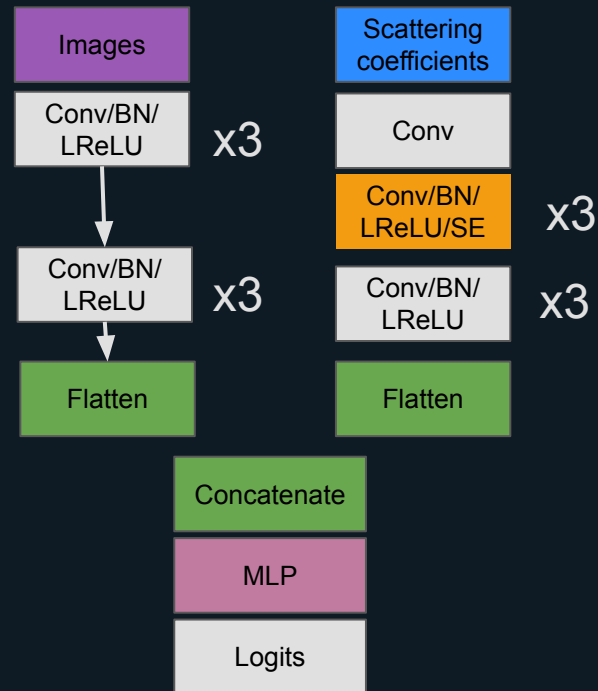
## Convolutional neural network (CNN)



## CNN-squeeze dual net (DualCSN)



## Scatter-squeeze dual net (DualSSN)



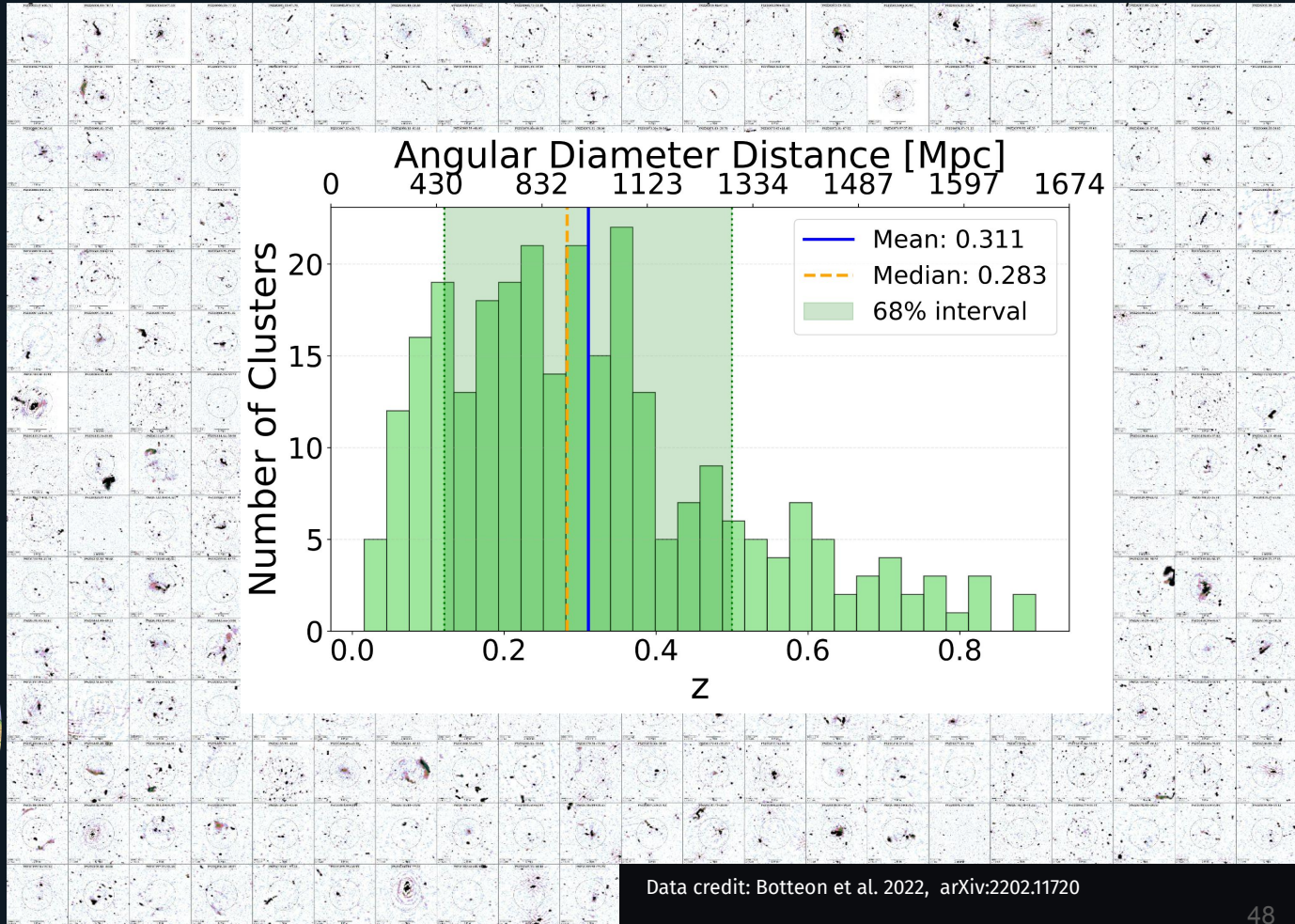
# Classification of diffuse radio emission from LoTSSDR2

# LOTSSDR2/PSZ2

LOFAR Two-metre Sky Survey  
Data Release (LoTSS-DR2)  
belonging to the second Planck  
catalogue of Sunyaev-Zel'dovich  
sources (PSZ2)

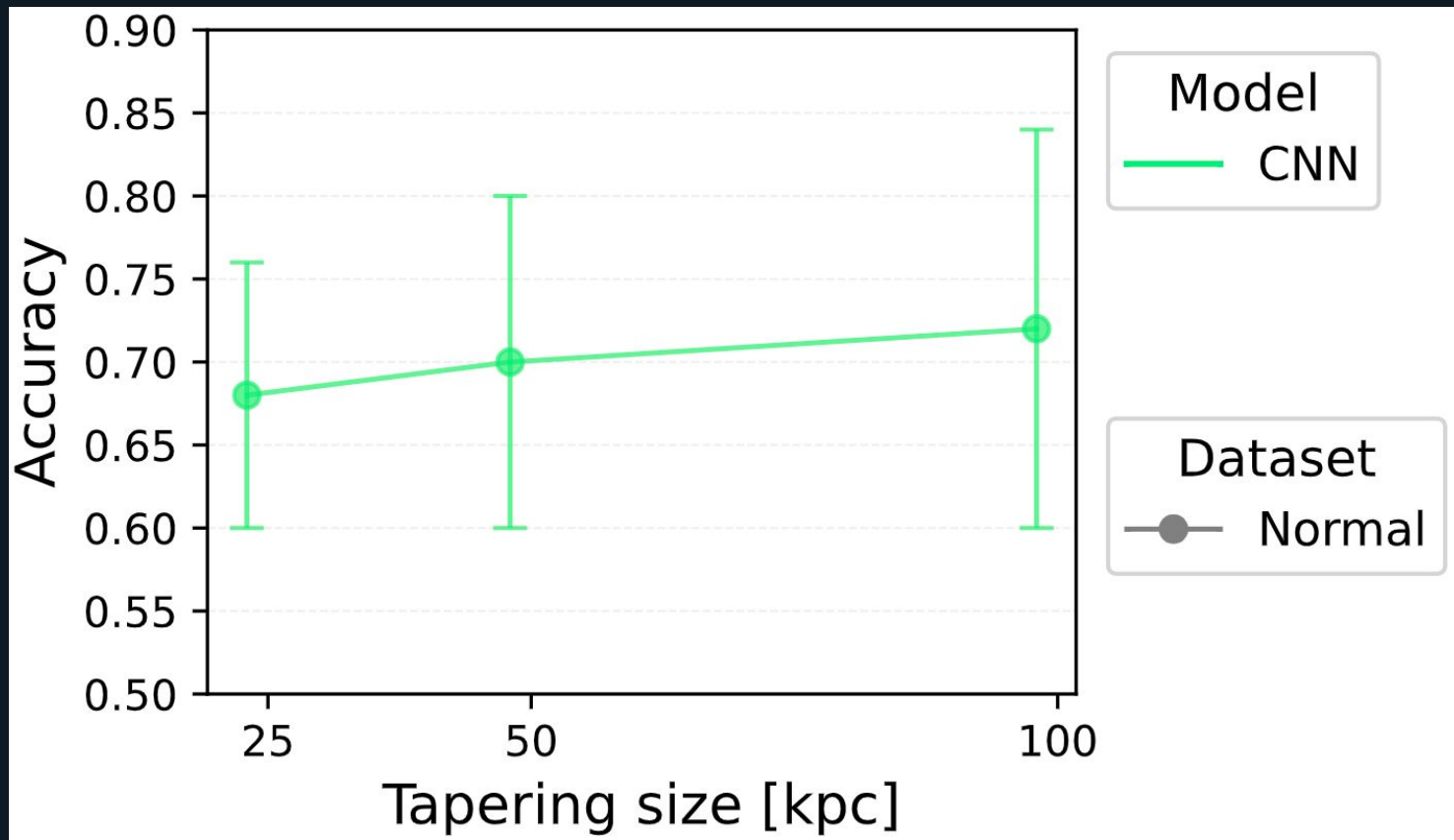
62 Diffuse Emission  
114 No Diffuse Emission

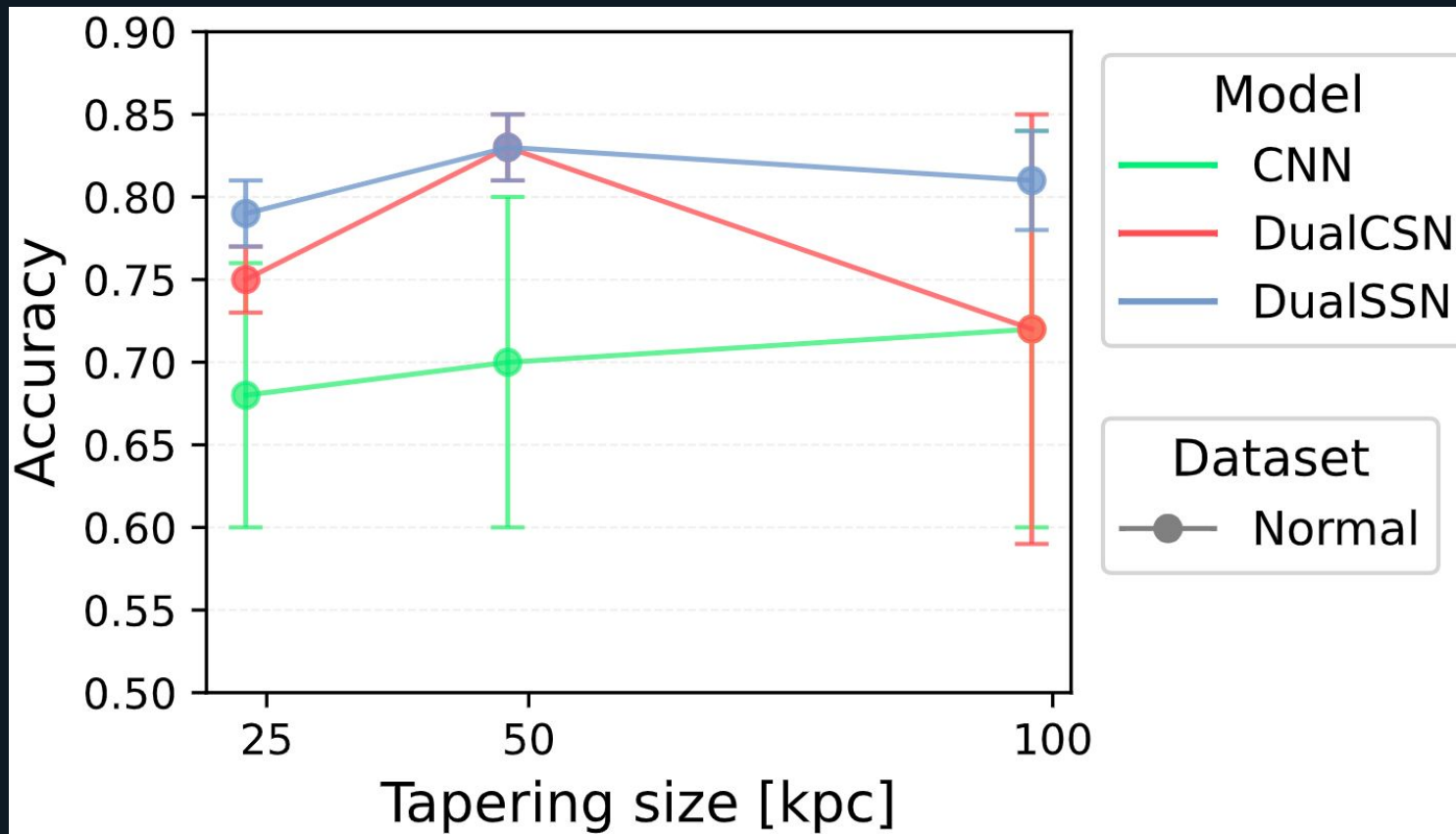
Processed to 1x128x128  
pixels

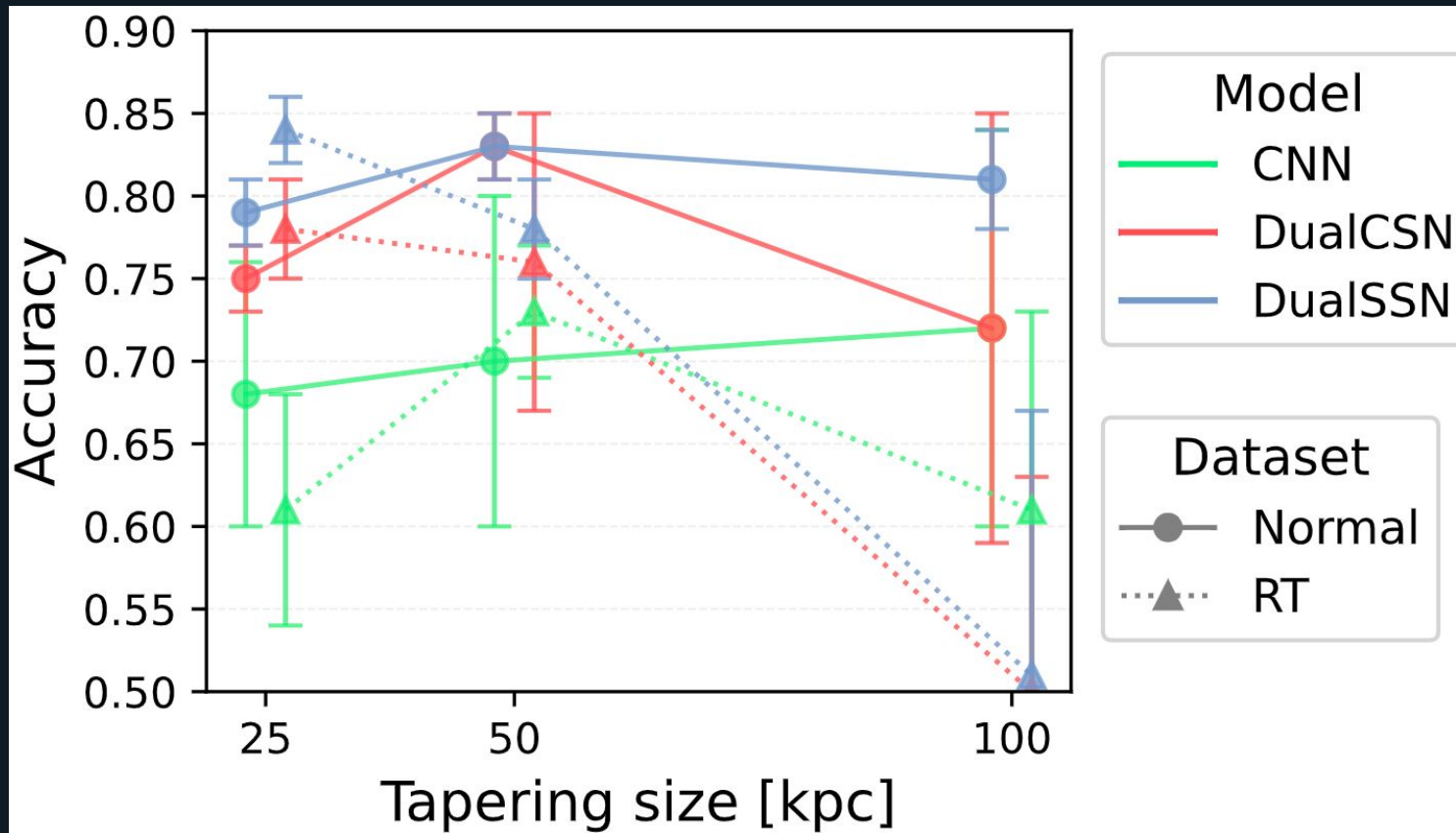


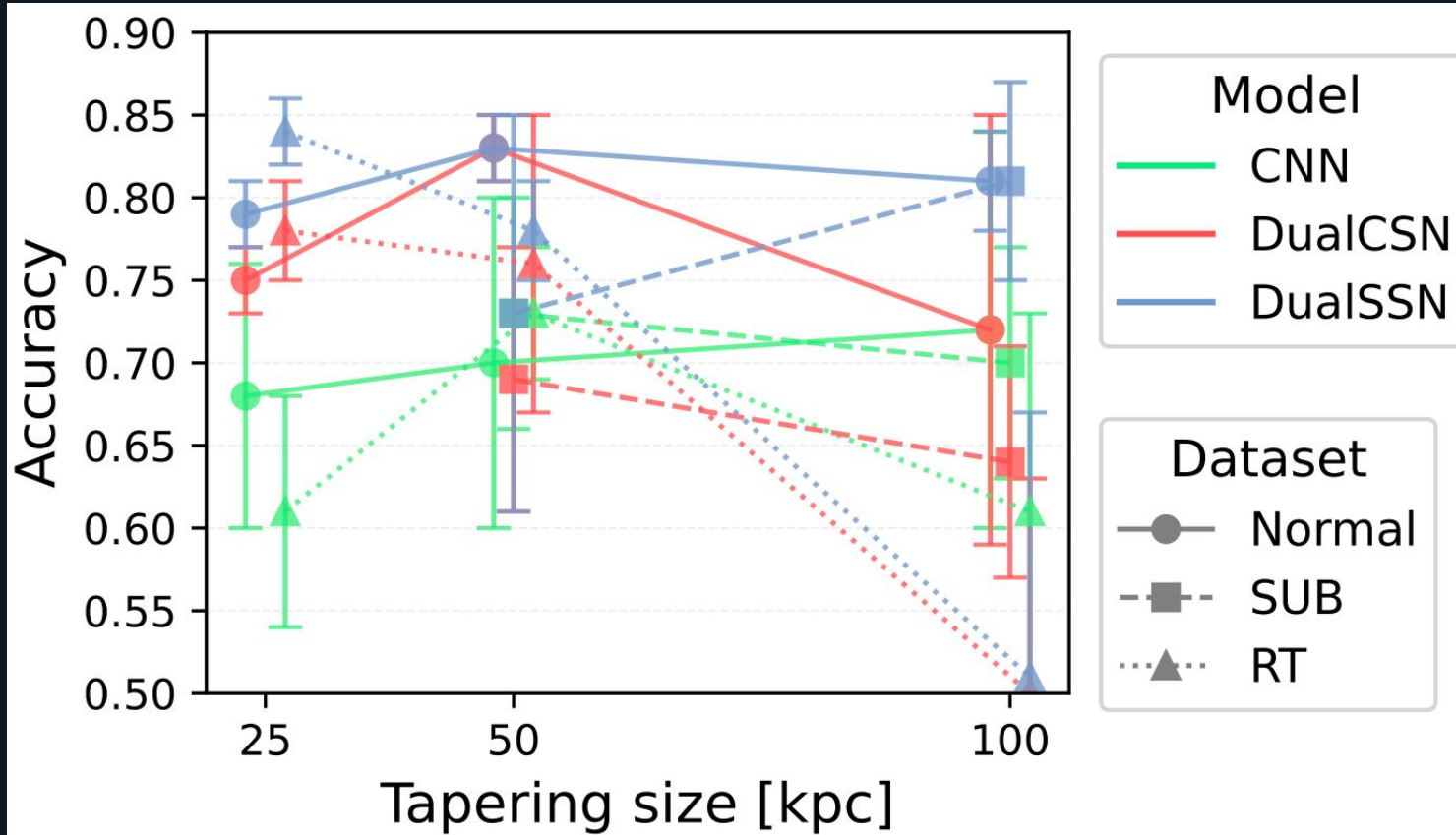
Data credit: Botteon et al. 2022, arXiv:2202.11720

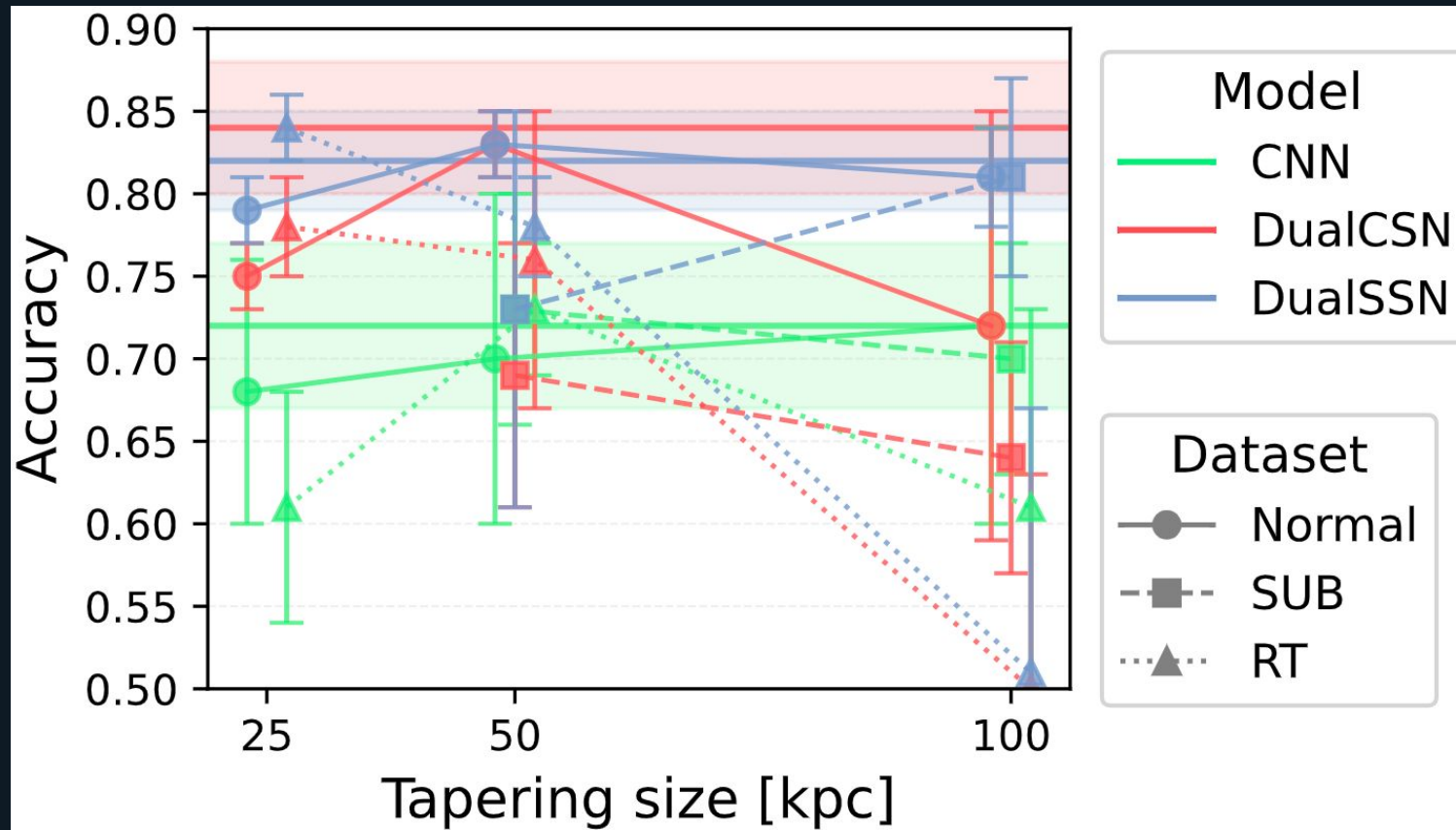
# Classification of diffuse radio emission from LoTSSDR2

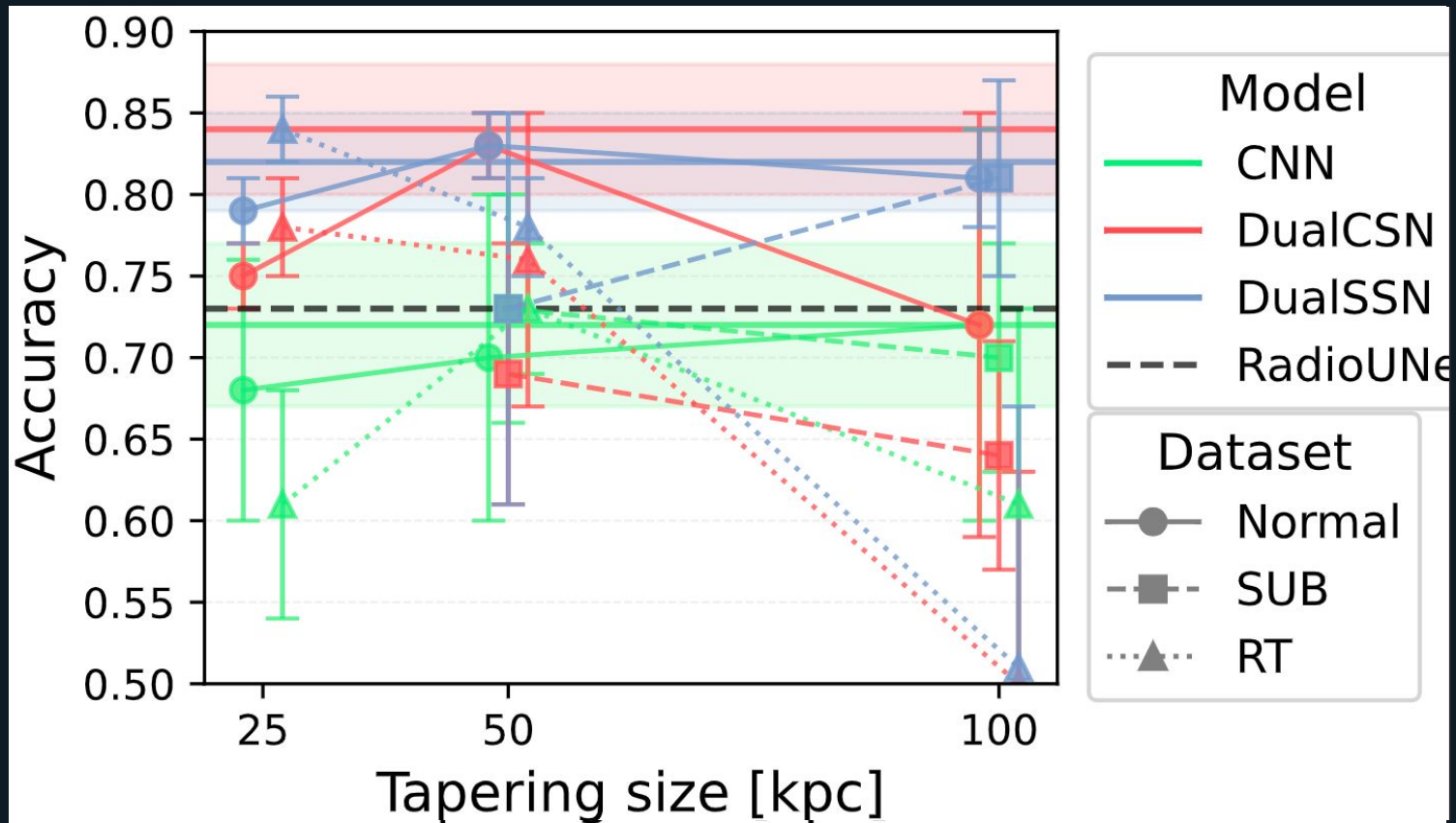






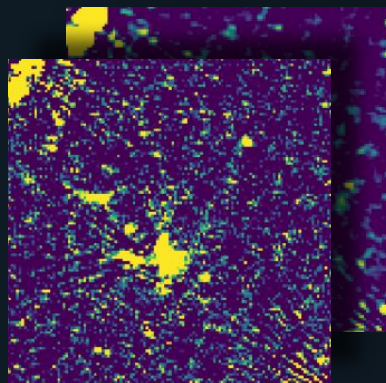






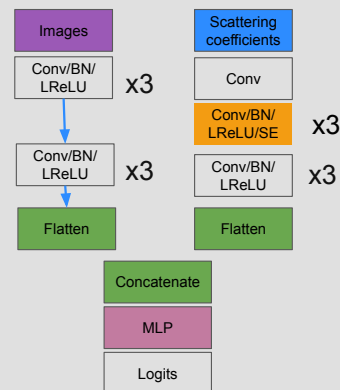
# Stacking images could render more information salient

Raw image

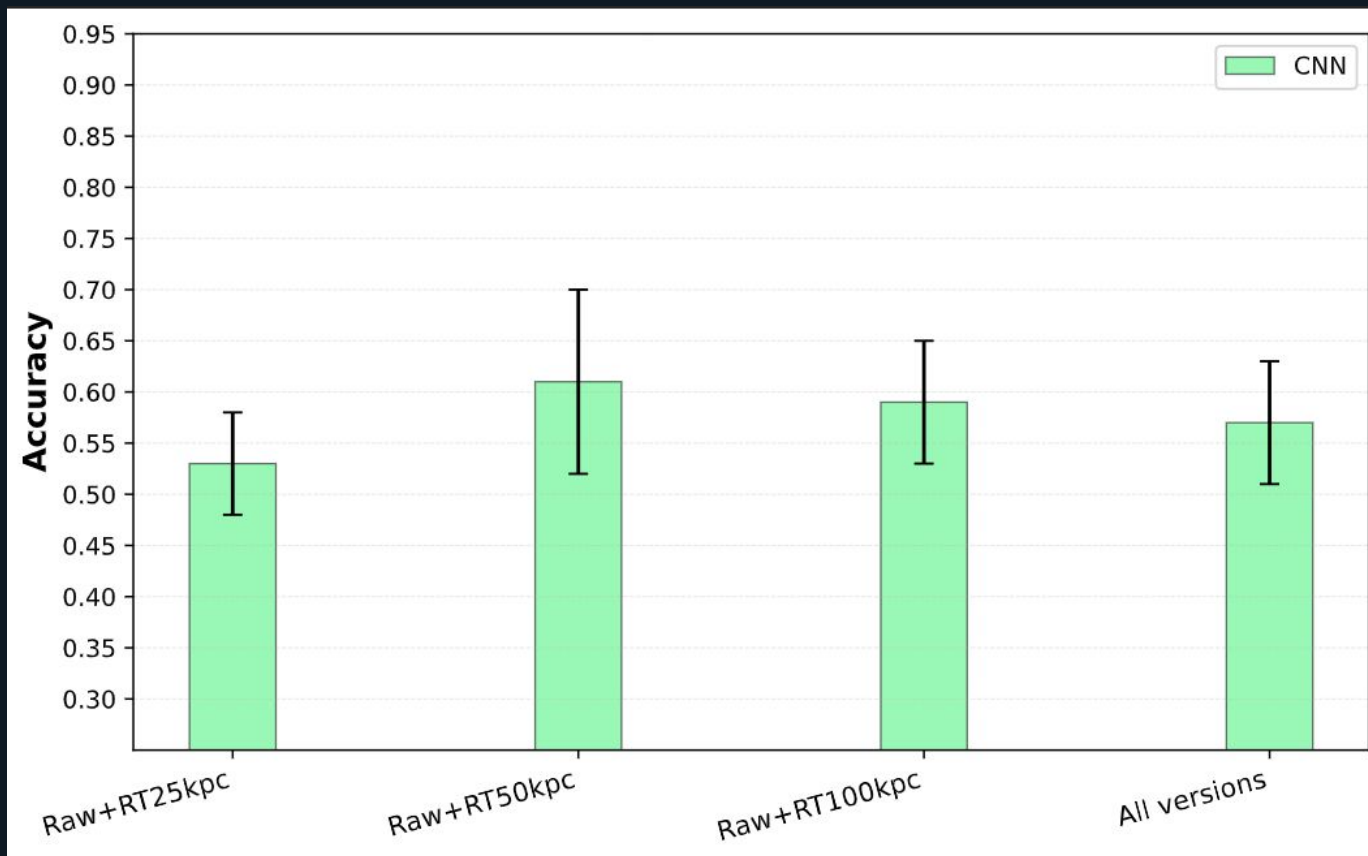


Tapered image

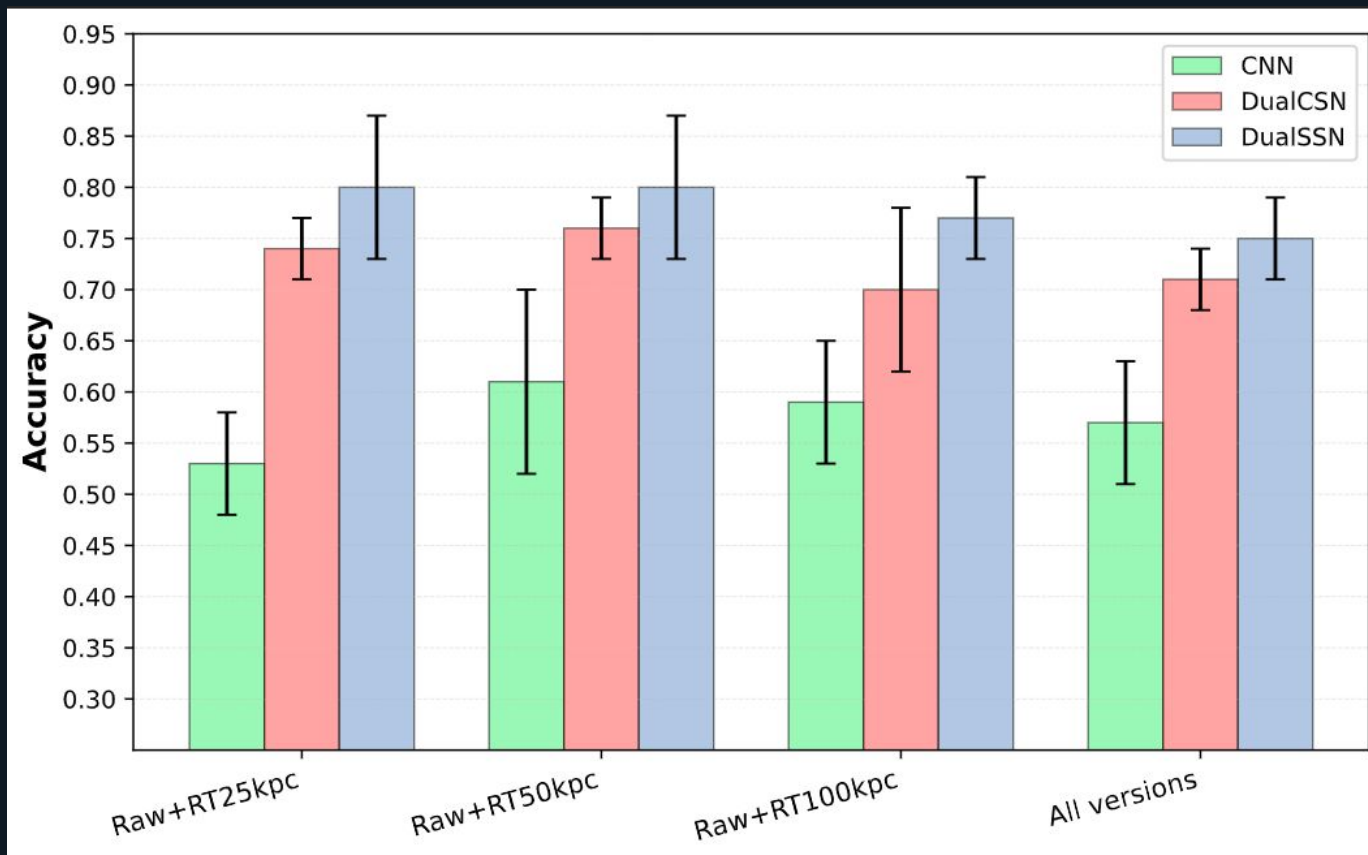
## DualSSN



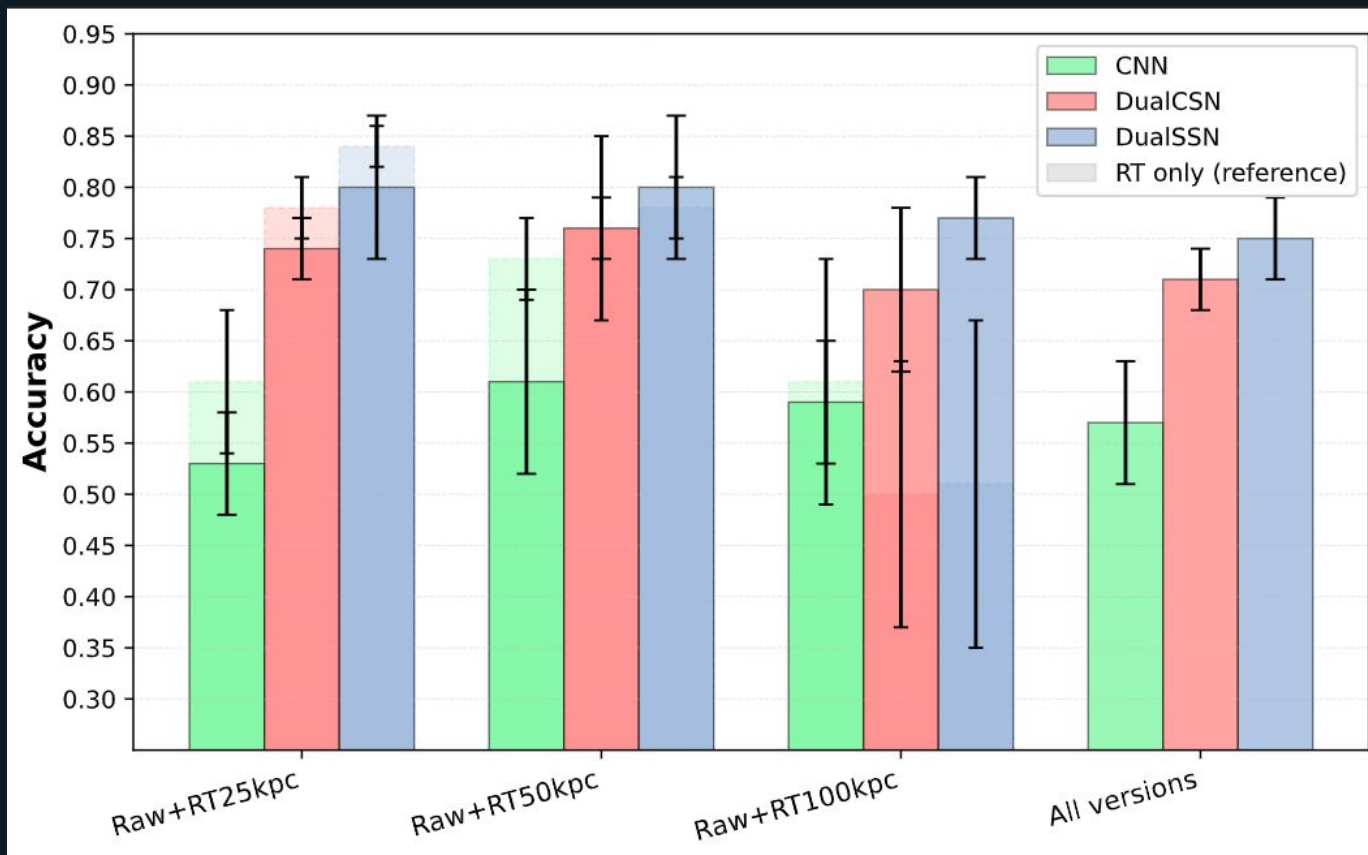
# Stacking images could render more information salient



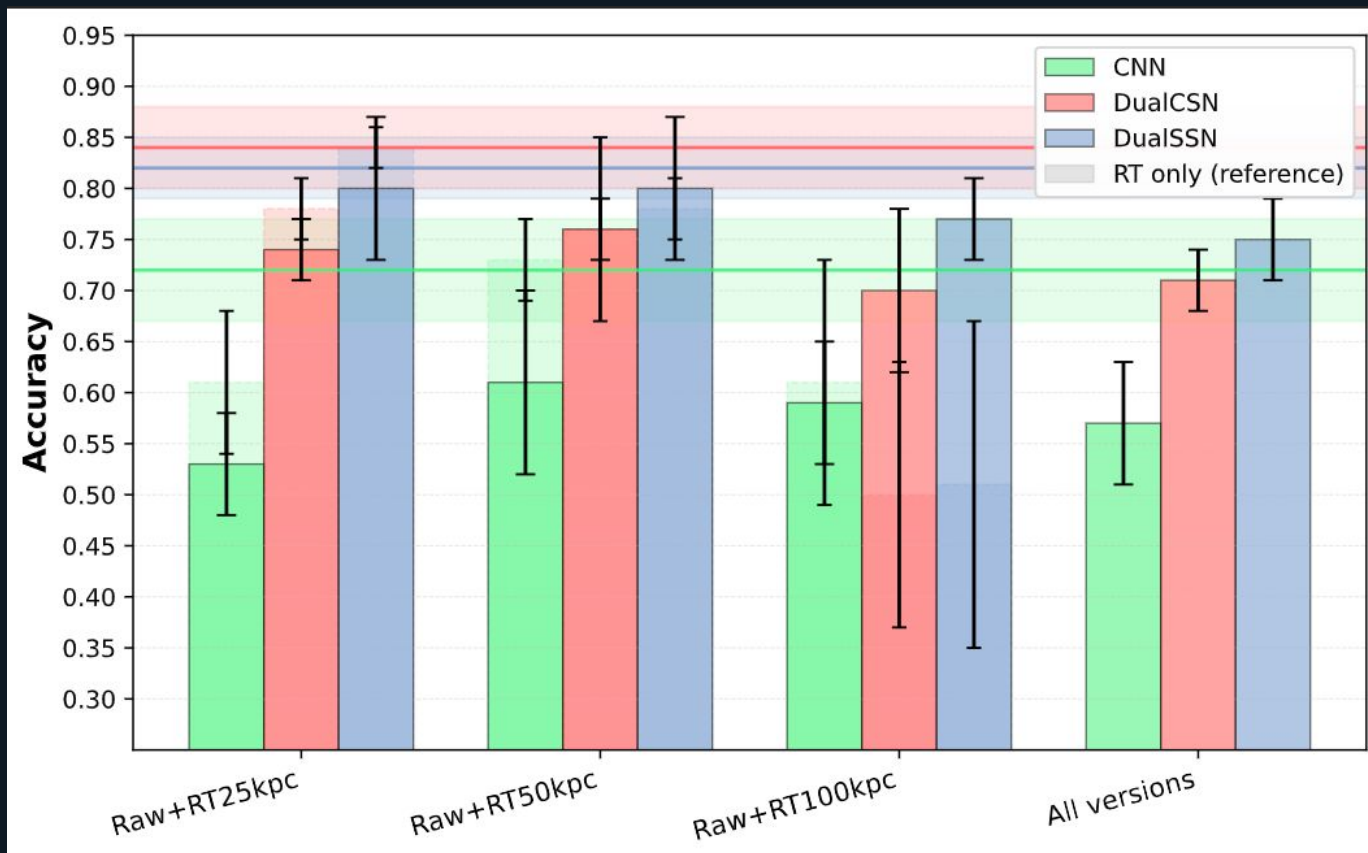
# Stacking images could render more information salient



# Stacking images could render more information salient



# Stacking images could render more information salient



## Conclusions and thank you

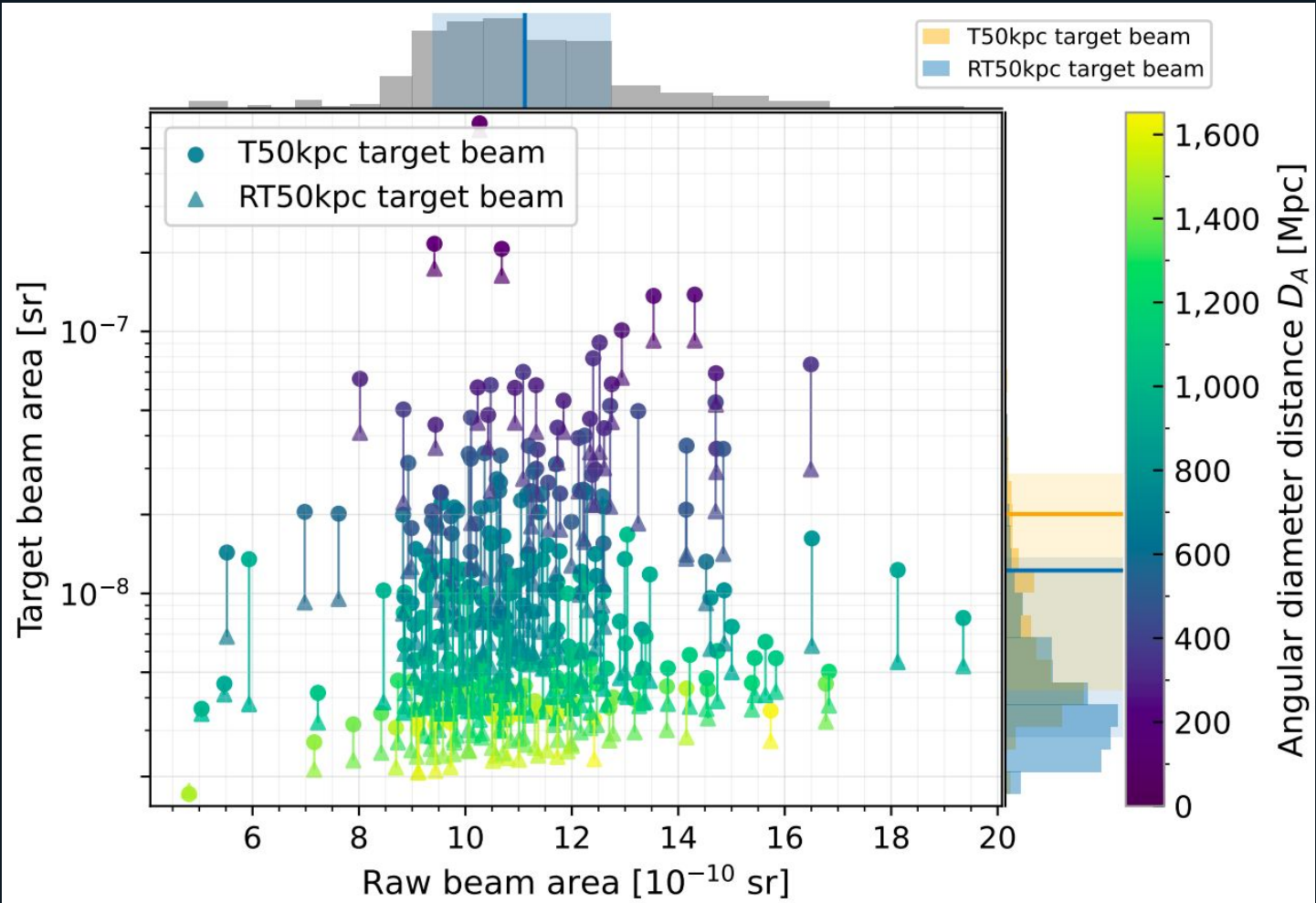
- The upcoming decennium can expect thousands of new discoveries of diffuse cluster radio emission
- Scattering transform, squeeze-excitation attention, and multi-branch architecture may all improve classification performance
- Tapering or blurring and stacking did not prove useful in this study

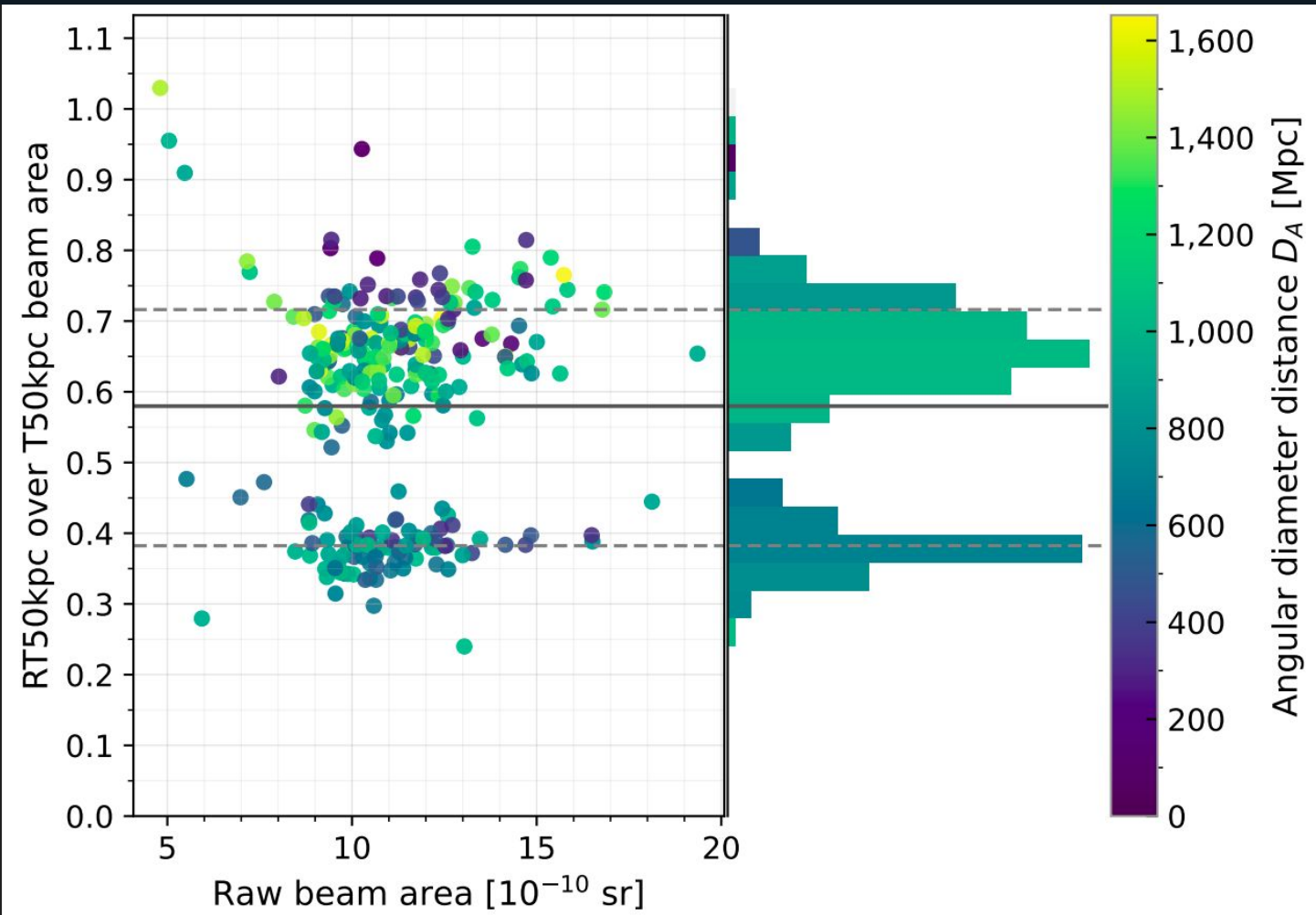
Thank you for your attention!

Bonus slides 1 -  
What more?

## Number of sources per class and data split for the two processing strategies

Class	Split	Constant FoV	Constant $n_{\text{beams}}$
DE	Train	46-51	41-46
	Validation	3-8	3-8
	Test	13	15
	TOTAL	67	64
NDE	Train	98-103	82-87
	Validation	9-14	6-11
	Test	28	21
	TOTAL	140	114
Total	–	207	178





# CNN classifier

Branch	Layer	Component	Depth	Activation	Regularizer	Parameters
Feature Extractor	1-2	5×5 Conv (s=2), BN	16	Leaky ReLU	Dropout2d (0.15)	448
	3-4	5×5 Conv (s=2), BN	32	Leaky ReLU	Dropout2d (0.20)	12,896
	5-6	5×5 Conv (s=2), BN	32	Leaky ReLU	Dropout2d (0.25)	25,696
	7-8	3×3 Conv (s=2), BN	48	Leaky ReLU	Dropout2d (0.30)	13,968
	9-10	3×3 Conv (s=2), BN	48	Leaky ReLU	Dropout2d (0.35)	20,880
	11-12	3×3 Conv (s=2), BN	64	Leaky ReLU	Dropout2d (0.40)	27,840
	13	AdaptiveAvgPool2d	64	-	-	0
Classifier	1-2	Flatten, Linear, BN	32	Leaky ReLU	Dropout (0.5)	2,144
	3	Linear	2	-	-	66
Total:						103,938

# DualCSN classifier

Branch	Layer	Component	Depth	Activation	Regularizer	Parameters
Image Encoder 1	1-2	5×5 Conv, BN	8	Leaky ReLU	Dropout2d (0.3)	208
	3-4	3×3 Conv, BN	16	Leaky ReLU	Dropout2d (0.3)	1,168
	5	2×2 MaxPool	16	-	-	0
	6-7	5×5 Conv, BN	32	Leaky ReLU	Dropout2d (0.4)	12,832
	8-9	3×3 Conv (s=2), BN	32	Leaky ReLU	Dropout2d (0.4)	9,248
	10-11	3×3 Conv (s=2), BN	32	Leaky ReLU	Dropout2d (0.4)	9,248
	12-15	2× [3×3 Conv (s=2), BN]	32	Leaky ReLU	Dropout2d (0.4, 0.5)	18,496
Image Encoder 2	1-2	3×3 Conv, BN, SE	32	Leaky ReLU	Dropout2d (0.3)	448
	3-4	3×3 Conv, BN, SE	32	Leaky ReLU	Dropout2d (0.3)	9,440
	5-6	3×3 Conv (s=2), BN, SE	32	Leaky ReLU	Dropout2d (0.3)	9,440
	7-8	3×3 Conv, BN, SE	32	Leaky ReLU	Dropout2d (0.4)	9,440
	9-10	3×3 Conv (s=2), BN, SE	32	Leaky ReLU	Dropout2d (0.4)	9,440
	11-12	3×3 Conv, BN, SE	32	Leaky ReLU	Dropout2d (0.5)	9,440
	13-14	3×3 Conv (s=2), BN, SE	32	Leaky ReLU	Dropout2d (0.5)	9,440
Classifier	1-2	Linear, BN	32	Leaky ReLU	Dropout (0.5)	278,624
	3-4	Linear, BN	32	Leaky ReLU	Dropout (0.5)	1,120
	5	Linear	2	-	-	66
Total:						388,530

# DualSSN classifier

Branch	Layer	Component	Depth	Activation	Regularizer	Parameters
Image Encoder	1-2	5×5 Conv, BN	8	Leaky ReLU	Dropout2d (0.2)	208
	3-4	3×3 Conv, BN	16	Leaky ReLU	Dropout2d (0.2)	1,168
	5	2×2 MaxPool	16	-	-	0
	6-7	5×5 Conv, BN	32	Leaky ReLU	Dropout2d (0.3)	12,832
	8-9	3×3 Conv (s=2), BN	32	Leaky ReLU	Dropout2d (0.3)	9,248
	10-11	3×3 Conv (s=2), BN	32	Leaky ReLU	Dropout2d (0.3)	9,248
	12-15	2× [3×3 Conv (s=2), BN]	32	Leaky ReLU	Dropout2d (0.3, 0.4)	18,496
Scattering Encoder	1-2	3×3 Conv, BN, SE	16	Leaky ReLU	Dropout2d (0.2)	24,384
	3-4	3×3 Conv, BN, SE	16	Leaky ReLU	Dropout2d (0.2)	2,352
	5-6	3×3 Conv (s=2), BN, SE	16	Leaky ReLU	Dropout2d (0.2)	2,352
	7-8	3×3 Conv, BN, SE	16	Leaky ReLU	Dropout2d (0.3)	2,352
	9-10	3×3 Conv (s=2), BN, SE	16	Leaky ReLU	Dropout2d (0.3)	2,352
	11-12	3×3 Conv, BN, SE	16	Leaky ReLU	Dropout2d (0.4)	2,352
	13-14	3×3 Conv (s=2), BN, SE	16	Leaky ReLU	Dropout2d (0.4)	2,352
Classifier	1-2	Linear, BN	32	Leaky ReLU	Dropout (0.5)	24,672
	3-4	Linear, BN	32	Leaky ReLU	Dropout (0.5)	1,120
	5	Linear	2	-	-	66
Total:						116,146

**Table B1.** Classification performance across datasets of CNN

Dataset	Accuracy	Precision	Recall	F1-score
RT25kpc	0.61 ± 0.07	0.54 ± 0.19	0.59 ± 0.23	0.55 ± 0.19
RT50kpc	<b>0.73 ± 0.04</b>	0.72 ± 0.08	0.61 ± 0.07	0.65 ± 0.03
RT100kpc	0.61 ± 0.12	0.56 ± 0.13	0.79 ± 0.14	0.63 ± 0.08
T25kpc	0.68 ± 0.08	0.60 ± 0.10	0.67 ± 0.12	0.62 ± 0.07
T50kpc	0.70 ± 0.10	<b>0.74 ± 0.14</b>	0.57 ± 0.15	0.61 ± 0.03
T100kpc	0.72 ± 0.12	0.67 ± 0.13	0.74 ± 0.13	0.68 ± 0.05
T50kpcSUB	0.73 ± 0.07	0.65 ± 0.08	<b>0.80 ± 0.25</b>	<b>0.70 ± 0.20</b>
T100kpcSUB	0.70 ± 0.07	0.58 ± 0.20	0.80 ± 0.28	0.67 ± 0.22

**Table B2.** Classification performance across datasets of DualCSN

Dataset	Accuracy	Precision	Recall	F1-score
RT25kpc	0.78 ± 0.03	0.77 ± 0.07	0.77 ± 0.07	0.77 ± 0.02
RT50kpc	0.76 ± 0.09	0.78 ± 0.12	0.67 ± 0.08	0.70 ± 0.06
RT100kpc	0.50 ± 0.13	0.47 ± 0.09	0.92 ± 0.04	0.61 ± 0.06
T25kpc	0.75 ± 0.02	0.67 ± 0.03	0.71 ± 0.06	0.69 ± 0.03
T50kpc	<b>0.83 ± 0.02</b>	<b>0.89 ± 0.08</b>	0.69 ± 0.08	0.77 ± 0.04
T100kpc	0.72 ± 0.13	0.61 ± 0.16	0.74 ± 0.26	0.64 ± 0.22
T50kpcSUB	0.69 ± 0.08	0.62 ± 0.06	<b>0.92 ± 0.04</b>	<b>0.74 ± 0.04</b>
T100kpcSUB	0.64 ± 0.07	0.59 ± 0.06	0.82 ± 0.10	0.68 ± 0.03

**Table B3.** Classification performance across datasets of DualSSN

Dataset	Accuracy	Precision	Recall	F1-score
RT25kpc	<b>0.84 ± 0.02</b>	<b>0.84 ± 0.04</b>	0.80 ± 0.04	0.82 ± 0.02
RT50kpc	0.78 ± 0.03	0.77 ± 0.06	0.68 ± 0.06	0.72 ± 0.04
RT100kpc	0.51 ± 0.16	0.50 ± 0.17	<b>0.95 ± 0.10</b>	0.63 ± 0.08
T25kpc	0.79 ± 0.02	0.73 ± 0.06	0.76 ± 0.11	0.74 ± 0.04
T50kpc	0.83 ± 0.02	0.85 ± 0.07	0.72 ± 0.08	0.77 ± 0.03
T100kpc	0.81 ± 0.03	0.76 ± 0.05	0.75 ± 0.14	0.74 ± 0.07
T50kpcSUB	0.73 ± 0.12	0.66 ± 0.10	0.94 ± 0.04	<b>0.77 ± 0.07</b>
T100kpcSUB	0.81 ± 0.06	0.77 ± 0.10	0.88 ± 0.07	<b>0.81 ± 0.04</b>

**Table C1.** Classification performance across datasets of CNN

Dataset	Accuracy	Precision	Recall	F1-score
Raw+RT25kpc	0.53 ± 0.05	0.51 ± 0.06	0.56 ± 0.23	0.49 ± 0.17
Raw+RT50kpc	<b>0.61 ± 0.09</b>	<b>0.60 ± 0.11</b>	<b>0.65 ± 0.13</b>	<b>0.61 ± 0.04</b>
Raw+RT100kpc	0.59 ± 0.06	0.55 ± 0.07	0.63 ± 0.12	0.58 ± 0.07
All versions	0.57 ± 0.06	0.54 ± 0.08	0.65 ± 0.17	0.57 ± 0.04

**Table C2.** Classification performance across datasets of DualCSN

Dataset	Accuracy	Precision	Recall	F1-score
Raw+RT25kpc	0.74 ± 0.03	<b>0.74 ± 0.08</b>	0.72 ± 0.08	0.72 ± 0.02
Raw+RT50kpc	<b>0.76 ± 0.03</b>	0.72 ± 0.04	<b>0.79 ± 0.05</b>	<b>0.76 ± 0.02</b>
Raw+RT100kpc	0.70 ± 0.08	0.67 ± 0.09	0.74 ± 0.06	0.70 ± 0.05
All versions	0.71 ± 0.03	0.70 ± 0.04	0.66 ± 0.10	0.67 ± 0.05

**Table C3.** Classification performance across datasets of DualSSN

Dataset	Accuracy	Precision	Recall	F1-score
Raw+RT25kpc	<b>0.80 ± 0.07</b>	<b>0.82 ± 0.14</b>	0.80 ± 0.10	<b>0.79 ± 0.05</b>
Raw+RT50kpc	0.80 ± 0.07	0.77 ± 0.10	<b>0.83 ± 0.07</b>	0.79 ± 0.06
Raw+RT100kpc	0.77 ± 0.04	0.76 ± 0.11	0.78 ± 0.09	0.76 ± 0.02
All versions	0.75 ± 0.04	0.76 ± 0.08	0.71 ± 0.15	0.72 ± 0.07

## Beam cropping proved important

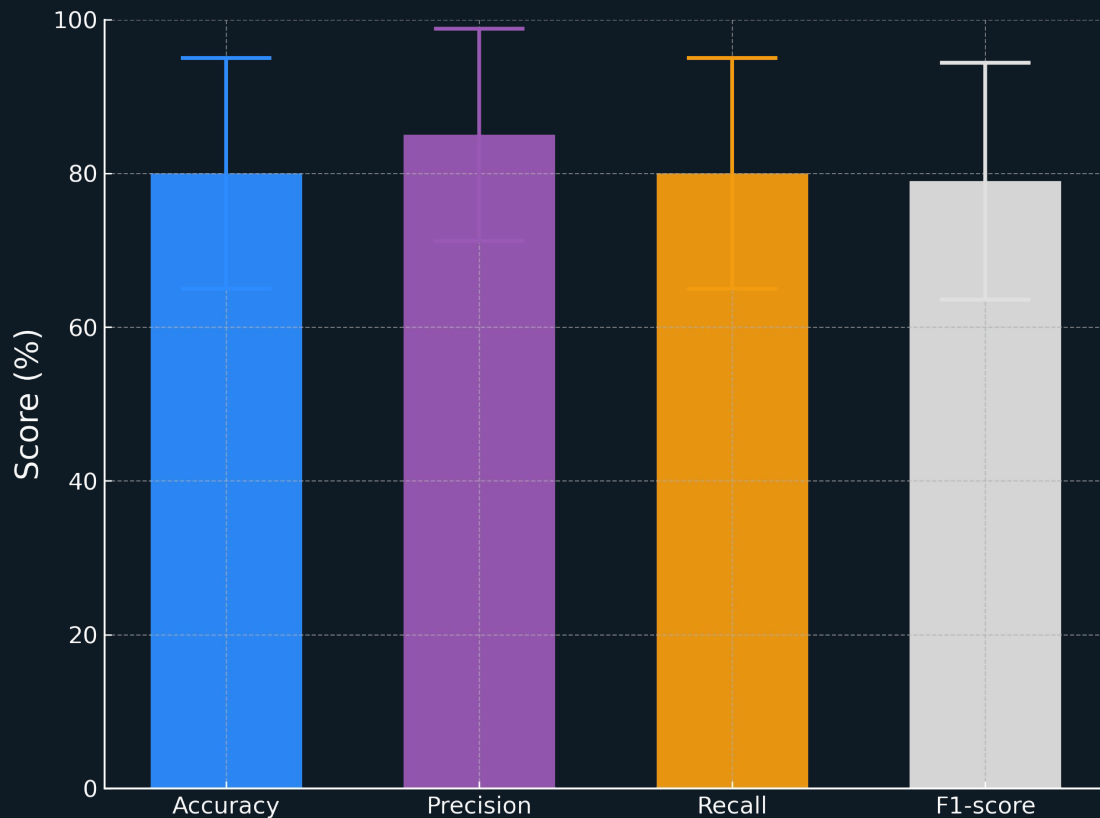
**Table 2.** Classification performance across four classifiers on raw data with percentile clipping and constant field of view.

Classifier	Accuracy	Precision	Recall	F1-score
CNN	$0.56 \pm 0.09$	$0.41 \pm 0.06$	<b><math>0.76 \pm 0.23</math></b>	$0.51 \pm 0.10$
DualCSN	$0.77 \pm 0.09$	$0.64 \pm 0.12$	$0.76 \pm 0.08$	$0.68 \pm 0.07$
DualSSN	<b><math>0.77 \pm 0.13</math></b>	<b><math>0.66 \pm 0.12</math></b>	$0.75 \pm 0.09$	<b><math>0.69 \pm 0.07</math></b>

**Table 3.** Classification performance across three classifiers on raw data with percentile clipping and beam-cropping.

Classifier	Accuracy	Precision	Recall	F1-score
CNN	$0.72 \pm 0.05$	$0.69 \pm 0.07$	$0.64 \pm 0.20$	$0.63 \pm 0.17$
DualCSN	<b><math>0.84 \pm 0.04</math></b>	$0.86 \pm 0.06$	<b><math>0.76 \pm 0.07</math></b>	<b><math>0.80 \pm 0.05</math></b>
DualSSN	$0.82 \pm 0.03$	<b><math>0.86 \pm 0.06</math></b>	$0.69 \pm 0.10$	$0.76 \pm 0.05$

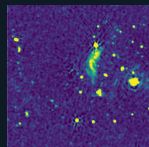
# Classify Radio Relics against Radio Halos



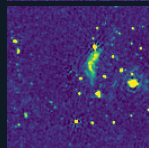
This plot  
is for T50

# The classification pipeline starts with processing of data

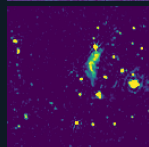
Cropping to  
(1, 512, 512)



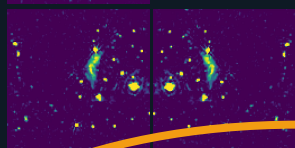
Downsample to  
(1, 128, 128)



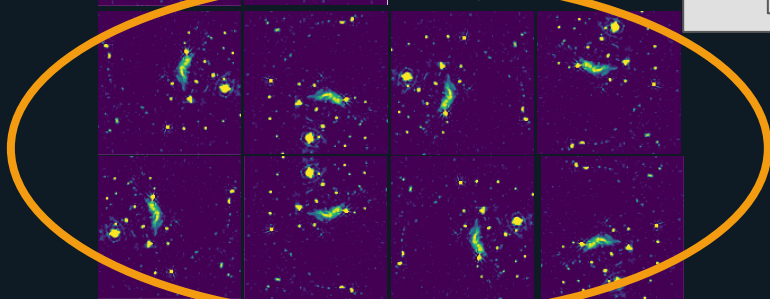
Normalisation



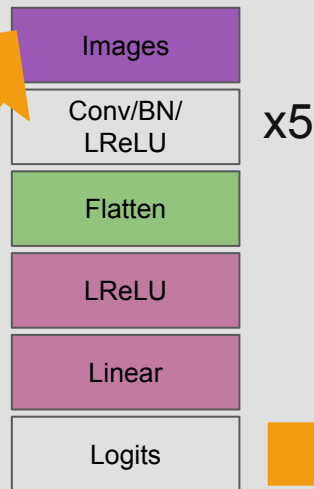
Horizontal  
flipping



Quarter turn  
rotations



## Convolutional Neural Network (CNN)

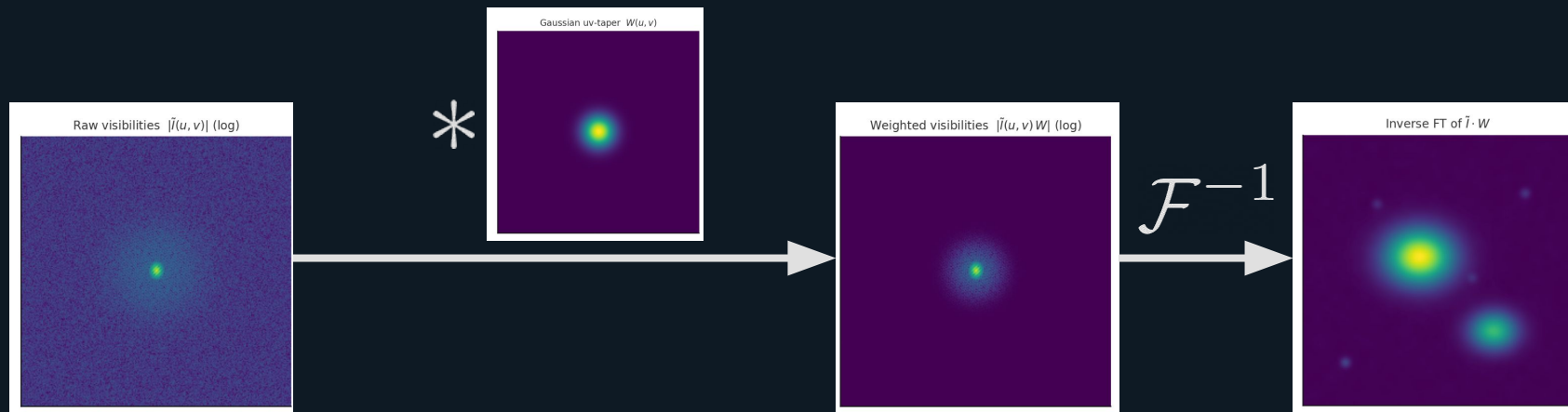


Average Accuracy: 77% ± 6%

	DE	NDE
DE	71% ±13%	29% ±13%
NDE	16% ±7%	84% ±7%
	DE	NDE
	Predicted Label	

Trained and  
evaluated  
model

# Tapering downweights longer baselines

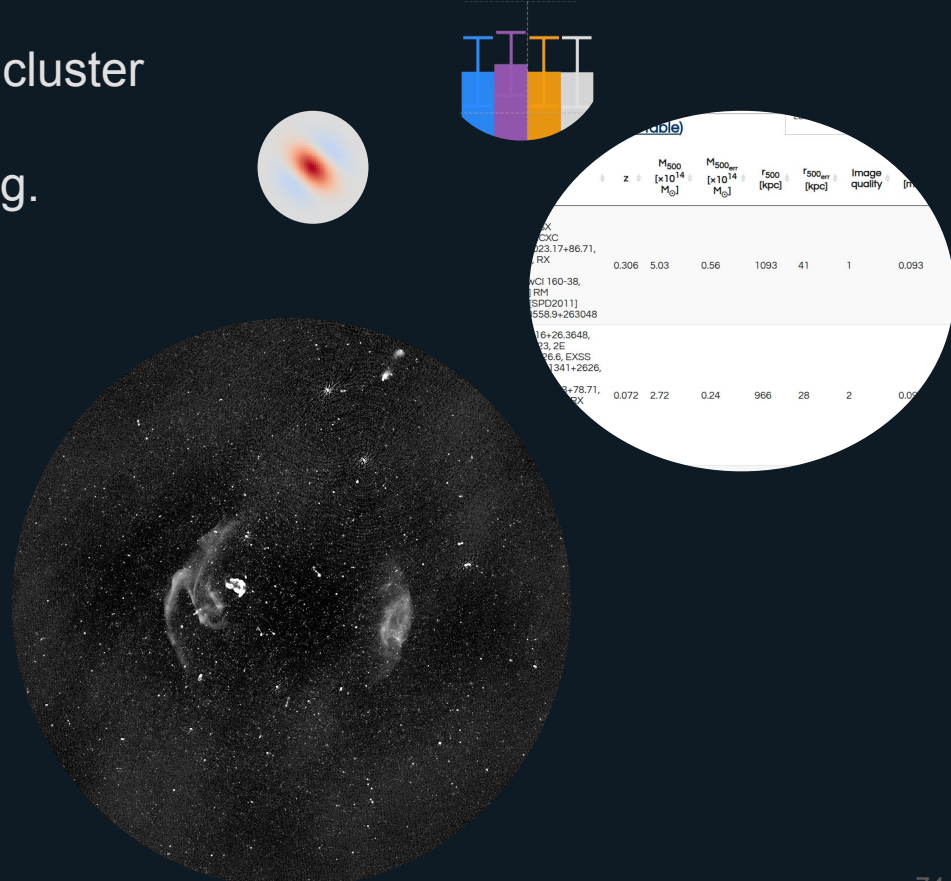


# Point source subtraction



# Future prospects

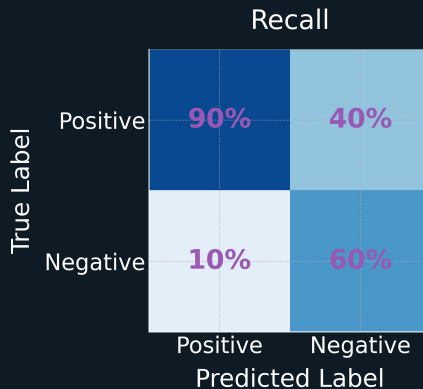
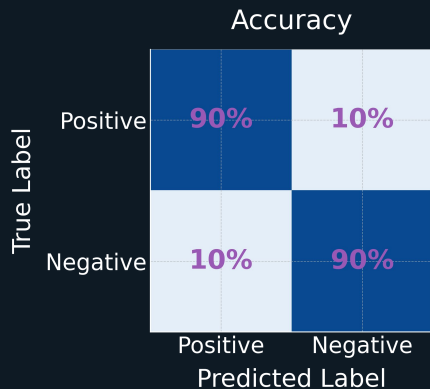
- Encode redshift, cluster mass, and cluster size as input
- Apply method on other datasets (e.g. MGCLS, MERGHERS)



# Bonus slides 2 - Machine learning technicalities

# The four horsemen of classification evaluation

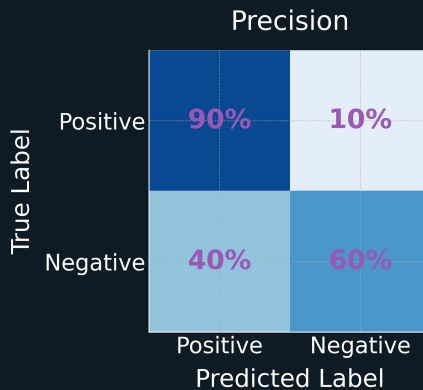
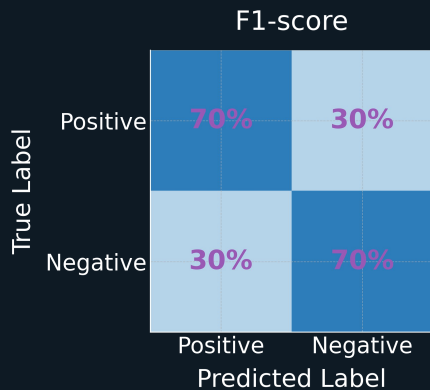
$$Accuracy = \frac{TP + TN}{TP + TN + FP + FN}$$



“Completeness”

$$Recall = \frac{TP}{TP + FN}$$

$$F1 = 2 \cdot \frac{Precision \cdot Recall}{Precision + Recall}$$



“Purity”

$$Precision = \frac{TP}{TP + FP}$$

# Scattering transforms are iterative wavelet transforms

$$\Psi_{J,L}(x) = [X, |X \star \psi_{j,\ell}|, ||X \star \psi_{j,\ell}| \star \psi_{j',\ell'}|]_{1 \leq \ell, \ell' \leq L, 1 \leq j < j' \leq J}$$

$$\phi_J(u) = 2^{-2J} \phi(2^{-J} u)$$

$$S_{J,L}(X) = \Psi_{J,L}(X) \star \phi_J$$

$$= [X \star \phi_J, |X \star \psi_{j,\ell}| \star \phi_J, ||X \star \psi_{j,\ell}| \star \psi_{j',\ell'}| \star \phi_J]_{1 \leq j < j' \leq J, 1 \leq \ell, \ell' \leq L}$$

$$X \star \phi_2 \quad |X \star \psi_{0,0}| \star \phi_2 \quad |X \star \psi_{0,1}| \star \phi_2 \quad |X \star \psi_{1,0}| \star \phi_2 \quad |X \star \psi_{1,1}| \star \phi_2 \quad ||X \star \psi_{0,0}| \star \psi_{1,0}| \star \phi_2 \quad ||X \star \psi_{0,0}| \star \psi_{1,1}| \star \phi_2 \quad ||X \star \psi_{0,1}| \star \psi_{1,0}| \star \phi_2 \quad ||X \star \psi_{0,1}| \star \psi_{1,1}| \star \phi_2$$



# Low pass filter for scattering transform

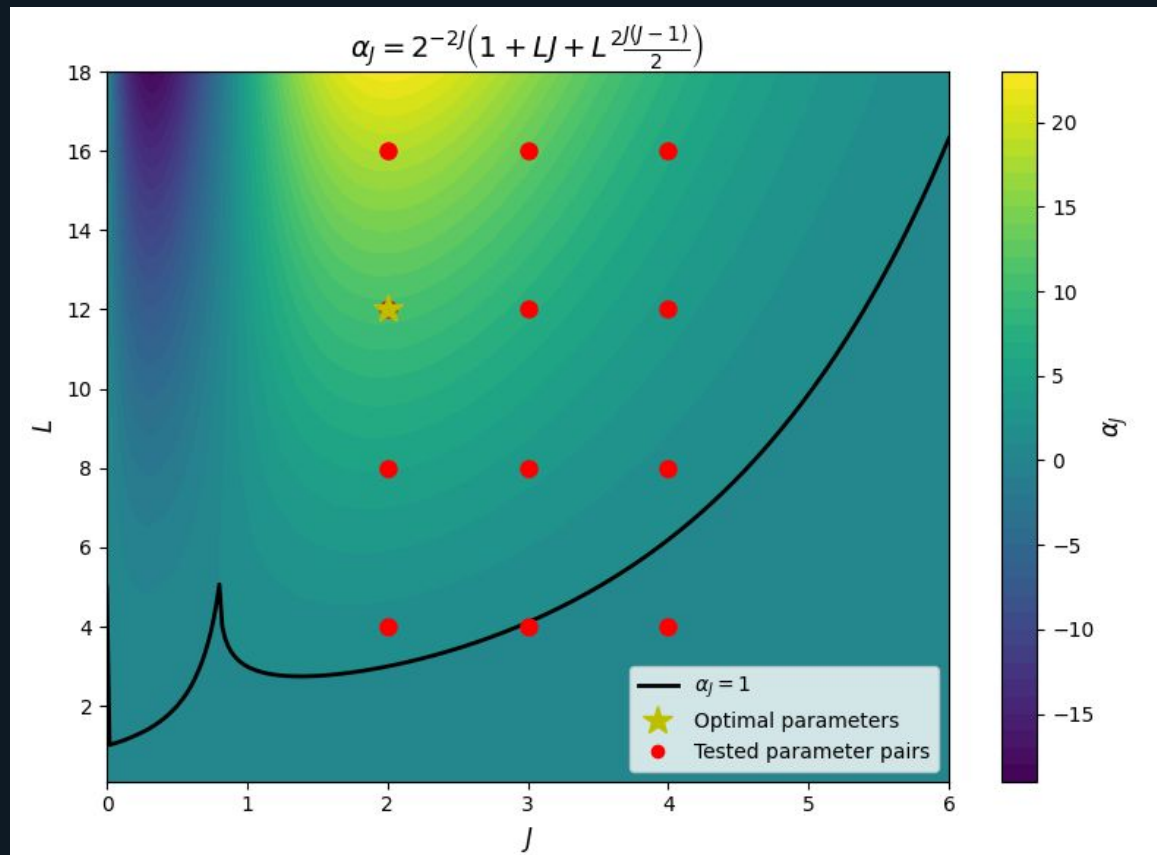
**Littlewood-Paley equality**  $\sum_{j=-\infty}^{+\infty} |\hat{\psi}(2^j \omega)|^2 = 1, \forall \omega > 0$   
Conservation of energy

**Capture lower frequencies of signal**  $[-2^{-J} \pi, 2^{-J} \pi]$

**With low-pass filter**  $\hat{\Phi}_J(\omega) = \left( \sum_{j=J+1}^{+\infty} |\hat{\psi}(2^j \omega)|^2 \right)^{1/2}$  **satisfying**  $\int \Phi_J(t) dt = 1$

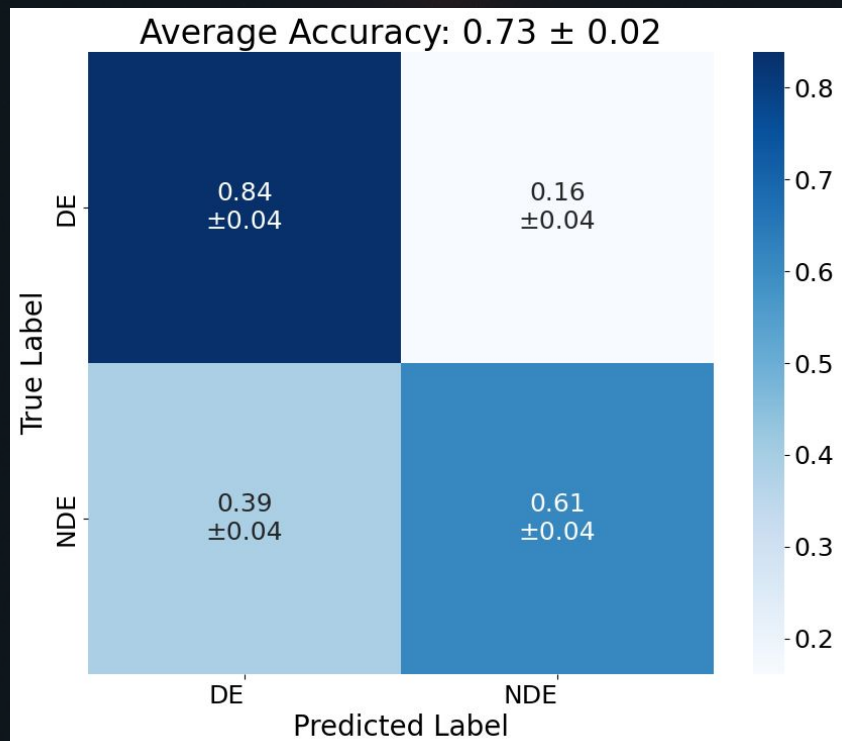
→ preserves norm and is therefore invertible

# Performance improves with number of scattering coefficients



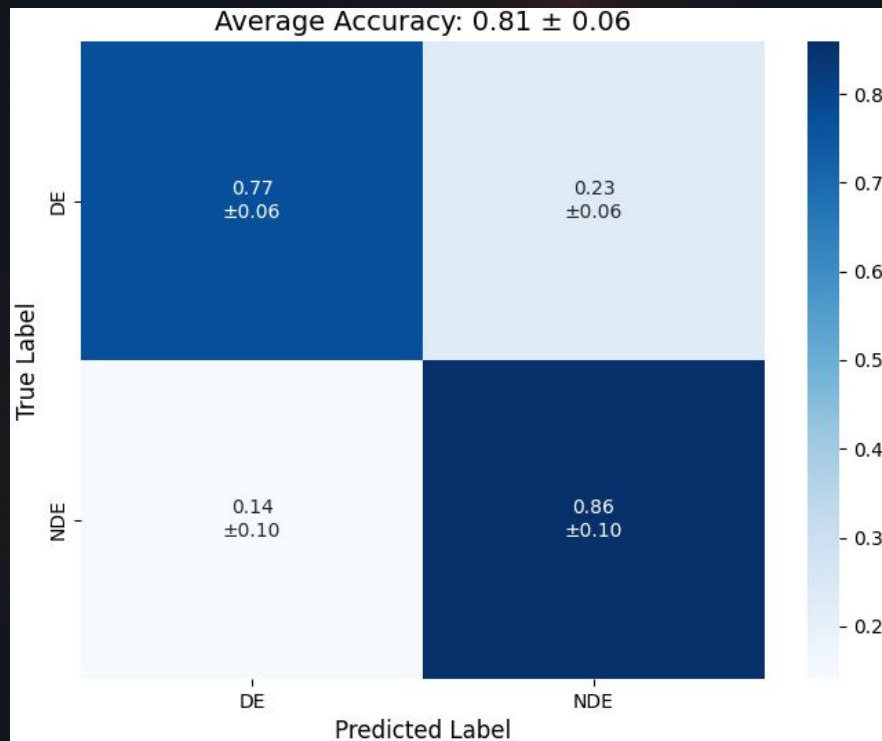
# Confusion matrices for classification of radio clusters (June 2025)

## MGCLS



CNN2: 8 layers, 2.5M parameters

## PSZ2



ScatterSqueezeDualNet: 14 + 2 layers, 3M parameters